

## Authors' Response to Anonymous Referee #1 Comments

The authors would like to thank the anonymous Referee for her/his comments that have helped us to improve this manuscript. Below, the major and minor comments are addressed by detailed point-by-point replies. Referee's comments are in blue and authors' replies in black.

### General comments

The paper presents a compilation of light scattering measurements obtained from a large number of aircraft campaigns, distributed globally, and they relate these measurements to ice crystal submicron complexity. This enables the authors to obtain estimates for the asymmetry parameter, a parameter of importance in NWP and climate modeling. They find from their analyses that the asymmetry parameter determination of 0.75 can be related to their complexity findings. This appears invariant with location and ice/cirrus formation, and the resulting scattering pattern results from the observed ice crystal complexity. As a consequence, this complexity expressed through the asymmetry parameter induces a not insubstantial-averaged further cooling effect not currently accounted for in climate models.

This is a largely well written paper, which links experimental results with theory and relates these measurements to ice crystal complexity and follows the theory through to an application in climate models. The paper provides nice results which deserve to be published, but the claim needs to be proven more rigorously with uncertainties attached to their estimates.

We thank the Referee for this positive general comment. In her/his comments the Referee has raised concerns on the rigour of the presented conclusions, especially on the uncertainties in the asymmetry factor. We acknowledge that the limitations of our measurements were not adequately discussed and have modified the discussion and conclusions to be more sensitive to these limitations. Below are listed the detailed replies to the Referee's major and minor comments.

### Major comments

1. The claim of the authors is that their measured PN angular scattering patterns are sufficient to determine the asymmetry parameter through some theoretical phase function that appears to fit through the data. This is not convincingly shown to be the case and appear to be eye fits at one single wavelength. There is no discussion in the text as to how the best fit to the measurements was statistically determined? Moreover, there are a number of extrapolations that could be used owing to the spread throughout the data, what uncertainty does this spread produce in the estimated asymmetry parameter values? There should be an uncertainty attached to their estimate of  $0.75 \pm ?$  Once these uncertainties have been derived for the asymmetry parameter, the uncertainty in the SWCRE should be consequently determined.

Estimating asymmetry factor from measurements that are covering only part of the angular region is challenging, especially since majority of the scattered intensity is found in the forward direction that is not covered by the measurements. We think that the best approach to estimate the asymmetry factor from the measurements is to use a physical model with a known asymmetry factor to fit the measurements in the known angular range, as done in this manuscript.

The same difficulty applies to estimating the uncertainty of the asymmetry factor if only part of the angular range is covered. For example, if we calculate the partial asymmetry factor for the angular range of 18 to 170° using the column aggregate model, we get an partial asymmetry factor of 0.14. This is approximately 20% of the total asymmetry factor of 0.75, since the forward peak contributes the majority part of the asymmetry factor. Even if we can estimate the uncertainty between the fit and the measurements in the restricted angular range, this uncertainty estimation contributes only 20% to the total uncertainty. Therefore, the measurements alone are not enough to estimate the uncertainty in the asymmetry factor, although it can be argued that the uncertainty of the asymmetry factor is the highest in the measurement region compared to the forward region, where the scattering intensity is mainly determined by the particle size and less of shape.

Owing to this discussion, we agree with the Referee that the discussions in the Sect. 3.4 and in the abstract and some of the conclusions are not well justified. Better than *retrieving* the

asymmetry factor from the measurements it is more justifiable to *compare* the different optical models to the measurements. Therefore, we have reformulated the Sect. 3.4 and the section title as “Comparison of the measured angular scattering functions to a light scattering database”. We have also omitted the sentence “*Using the severely roughened hexagonal aggregate model asymmetry factors of 0.750 and 0.754 at 532 nm and 804 nm, respectively, were retrieved*” and instead write in the Sect. 4: “*the severely roughened hexagonal aggregate model has relatively low asymmetry factors of 0.750 and 0.754 for 532 nm and 804 nm, respectively*”. The abstract we have modified so that instead of writing: “*as a consequence, a low asymmetry factor of 0.75 is observed*”, we write “*as a consequence, a similar flat and featureless angular scattering function is observed. A comparison between the measurements and a database of optical particle properties showed that severely roughened hexagonal aggregates optimally represents the measurements in the observed angular range*”.

We also make a stronger case in the Sect. 3.4 that the severely roughened hexagonal aggregate model best represents our measurement. We have added a new figure that compares the different models with the measurements at 804 nm (please see answer to comment 2) and justify the fit by calculating the root mean square errors (RMSE) between the model and the mean of the measurements. For both wavelengths the column aggregate model has the lowest RMSEs of 0.0017 and 0.0014 (for 532 and 804 nm, respectively) compared to the other models (RMSE between 0.0022 and 0.0111 for 532 nm, and 0.0037 and 0.0208 for 804 nm). The discussion of the RMSE analysis was added to the Sect. 3.4.

The asymmetry factors around 0.75 are, therefore, not *retrieved* from the measurements but represent the asymmetry factor of the severely roughened hexagonal aggregate model. This asymmetry factor is fixed for a given size distribution. Later, we use the severely roughened hexagonal aggregate model for deriving the parameterization of SW asymmetry factors for the ECHAM-HAM model. We believe this approach is still justified based on the microphysical observations. However, we agree that the claim in the last sentence of the first conclusions paragraph is not well justified and this conclusion is rewritten in the revised version (please see the reply to comment 3).

2. The other wavelength of 0.804  $\mu\text{m}$  is only once shown, the same as Figure 5 should be shown but for 0.804  $\mu\text{m}$  using all models. Moreover, the eight-column aggregate shown at 0.804  $\mu\text{m}$ , is only just within the measured uncertainties at side scattering angles. This could be owing to the aspect ratio of the monomer columns not being sufficiently large and spaced out more than the compact model they show. The aspect ratio is also an important determinant of the asymmetry parameter as shown by Fu (2007), among others. It would be interesting to plot the approach of Fu (2007), to see if that treatment provides similar low values to those being estimated from the data.

We added a new figure (Fig. 6) showing a comparison between the PN measurements and different models results calculated for 804 nm. This comparison shows that from all of the different habit models, the severely roughened column aggregate model has the best overall agreement with the measurements at 804 nm. Other models underestimate the backscattering intensity from 120° onwards. A discussion of this comparison was added in Section 3.4.

The Referee also suggests to modify the aspect ratio of the severely roughened column aggregate model in order to find a better fit to the measurements at the 804 nm wavelength, as done in the work of Fu (2007). Fu (2007) has showed that modifying the aspect ratio will influence the asymmetry factor of single hexagonal columns. We agree that modifying the aspect ratio of the severely roughened column aggregate model to create a better fit at 804 nm would be an interesting investigation. However, modifying the existing optical particle model or introducing new optical models is not the scope of this paper for two reasons. First, the focus of this paper is to present globally distributed observations of ice crystal mesoscopic complexity and relate them to the angular light scattering measurements. The modelling efforts in this paper are used as a tool to understand the implications of the measurement results. We hope that the measurements will inspire to development of new optical particle models in the future. Secondly, we do not have enough spectral information on the angular scattering functions that we can justify using different optical models for different wavelength bands. We think that the best approach here is to use one optical model to calculate the asymmetry factors for all the SW bands. The use of the severely

roughened column aggregate model is justified since it provides the best overall fit on both wavelengths.

3. The paper concludes that it is appropriate to apply the eight-column aggregate in climate and weather models. This is a rather significant claim as the model has only been tested at one single wavelength, at 0.805  $\mu\text{m}$ , it does not appear to possess the correct absorption properties at side scattering angles for the possible reasons stated above. It is unclear as to how this model would fit observations at other wavelengths of importance, such as in the terrestrial window region, far infrared, and at more absorbing solar wavelengths, such as at 1.6 and 2.2  $\mu\text{m}$ . These wavelengths are also of importance in weather and climate modelling. The authors present no evidence to support their general claim.

We agree that the spectral consistency of optical particle models is one of the biggest challenges in current climate models and in remote sensing retrievals. Modelling the spectral dependency of the asymmetry factor is difficult, since atmospheric measurements are available in only few wavelengths. Additional challenge is posed through the fact that each of the operated polar nephelometer work at a single wavelength, and therefore, combining the polar nephelometric measurements to gain spectral information will inevitably contain uncertainties merging from different measurement setups. For example, in our case we cannot completely distinguish, which proportion of the difference we see between the measurements and the model are real and which is contributed by the measurement setup, different calibration procedures, etc.

We agree that the spectral uncertainty of the asymmetry factors is not adequately discussed in the text. To correct this, we modified the section 4.1 and added the following discussion at the beginning of the section:

*“Fig. 4 showed that the observed high degree of mesoscopic scale complexity dominates the angular scattering function over the ice crystal shape and a uniform angular scattering function is observed at two wavelengths (532 and 804 nm). Therefore, it is justified to use a single-habit optical ice particle model assuming severely roughened surfaces to compute the bulk optical properties of ice clouds. It was found that the severely roughened column aggregate model showed the best fit of the atmospheric measurements performed at both wavelengths. At 804 nm the model disagreed slightly with the measurements at the sideward angles (Fig. 4). This disagreement indicates that either the severely roughened column aggregate model does not accurately represent the spectral dependence of the asymmetry factors, or could also be related to systematic measurement uncertainties caused by using different measurement systems. However, since we only have information on the ice particle angular scattering properties at two wavelengths at the moment, only one optical particle model is used to parameterize the asymmetry factors.”*

We also changed the last sentence in the first paragraph of the conclusions: *“Moreover, since the ice particle angular scattering functions did not vary significantly between different geographical locations, the modelling efforts of ice particle optical properties in future weather forecast and climate models will be simplified.”*

4. A further point about Figure 5 also needs to be noted. Recent theoretical electromagnetic studies have shown that surface roughness, at scattering angles around exact backscatter, induces coherent backscattering, so the phase functions of surface roughened ice should not apparently be flat at exact backscattering angles, there ought to be some backscattering amplitude present. The authors are referred to the following paper for further information about this interesting interference effect, [https://www.osapublishing.org/DirectPDFAccess/B8203150-AE8E-68E9-D2CB7062A1AB5EF8\\_385794/oe-26-10-A508.pdf?da=1&id=385794&seq=0&mobile=no](https://www.osapublishing.org/DirectPDFAccess/B8203150-AE8E-68E9-D2CB7062A1AB5EF8_385794/oe-26-10-A508.pdf?da=1&id=385794&seq=0&mobile=no). To compute the phase functions, the authors use a database which probably applies the improved physical optics approximation, in that multiple scattering is not included, so surface roughness is approximated by some geometrical treatment such as facet tilting to smooth the phase functions that appear in Figure 5. As a consequence of this, one could argue that the phase functions presented in Figure 5 are incorrect. Of course, owing to the asymmetry parameter being largely determined by diffraction, its derived value will not be much affected by this backscattering amplitude. However, this still does need to be noted in my opinion to encourage inclusion of multiple scattering in calculating the phase functions,

especially if they are to be used for lidar applications at visible wavelengths. However, to obtain more representative phase functions, the backscattering amplitude could be added on to the phase functions presented in Figure 5. There is a parameterization that the authors could use to do this as explained in this paper <https://www.osapublishing.org/oe/abstract.cfm?uri=oe-24-1-620>, where IGOM is corrected using the estimated amplitude obtained from electromagnetic calculations.

The Referee points out that recent theoretical electromagnetic studies have shown that surface roughness can lead to coherent backscattering enhancement at angles around exact backscattering whereas the theoretical functions of severely roughened particles showed in Figs. 5 and 6 do not take into consideration this effect. However, for the aspect of energy redistribution in the scattering process the backscattering enhancement has a negligible effect - as also stated by the Referee and, thus the derived asymmetry factor will not be affected through exclusion of this effect. The Referee also pointed out that this effect can have consequences for lidar application, which we agree. Therefore, we added a discussion of this effect to the Chapter 3.4:

*“At the angles around exact-backscattering the severely roughened column aggregate model predicts a relatively flat behaviour. However, recent modelling studies have indicated that the scattering intensities around exact backscattering angles should be enhanced due to coherent scattering (e.g. Zhou, 2018). Although this effect can be important for lidar applications, it does not significantly affect the redistribution of the energy in the scattering process and, thus, the magnitude of the asymmetry factor.”*

Furthermore, the Referee states that it is arguable that the theoretical phase functions in Figs. 5 and 6 are incorrect due to the treatment of the surface roughness in the model by using the tilted-facet (TF) method. Although the TF method may not accurately represent the physical surface roughness, it has been shown that the TF method can be used to model the phase matrix element P11 with high accuracy (Liu, Panetta and Yang, 2013). Also, arguing whether an optical particle model is incorrect is usually based on comparison of models with more sophisticated models, rarely on a comparison with measurements. This study presents an comparison of one optical data base with atmospheric measurements. In future, it is certainly of interest to perform more such comparisons with also other optical particle models to address the question of which optical models perform the best for different applications.

5. Also, for some reason, the authors do not cite papers prior to 2010, there are some, but these are few and far between and tend to be their own. This needs to be corrected.

We have expanded the list of cited papers. Please refer to answers to minor comments 2, 3, 9, 20 and 21.

Minor comments now follow:

1. In the abstract, the averaged asymmetry parameter of 0.75 is determined at the wavelength of? We added wavelength after the asymmetry factor.

2. Introduction line 15, similar results by Ulanowski et al., (2006) and Ulanowski et al. 2014 were also reported.

We added citation to Ulanowski et al. (2016) and Ulanowski et al. 2014 to line 15.

3. Introduction line 16, representations of ice crystal surface roughness via facet tilting were also added prior to 2008 by Macke et al. (1996)[ <https://journals.ametsoc.org/doi/pdf/10.1175/1520-0469%281996%29053%3C2813%3ASSPOAI%3E2.0.CO%3B2>], Yang and Liou (1998) [Single-scattering properties of complex ice crystals in terrestrial atmosphere, *Contr. Atmos. Phys.*, 71, 223–248, 1998], Baran et al. (2001)[ <https://rmets.onlinelibrary.wiley.com/doi/abs/10.1002/qj.49712757711>], Baran and Francis (2004)[ <https://rmets.onlinelibrary.wiley.com/doi/10.1256/qj.03.151>], Sun et al. (2004)[ <https://www.osapublishing.org/ao/abstract.cfm?uri=ao-43-9-1957>]. There are of course others.

We added both the citations to Macke et al. (1996), Yang and Liou (1998), Baran et al. (2001), Baran and Francis (2004) and Sun et al. (2004) and “e.g.” before the citations.

9. Page 2, discussion on polarization, line 2, The

same was also shown by Baran and Labonnote [<https://www.sciencedirect.com/science/article/pii/S0022407305003699>] in regards to polarization.

We added this reference.

10. Page 3, line 15, replace “in” by “on”.

We corrected this.

11. Page 3, line 25, perhaps, the word “the” needs to be incorporated before “discrete dipole”.

We added “the”.

12. Page 3, line 34, insert the word “to” before “as”. . .

We corrected this.

13. Section 2.2, in the discussion on the PN being used to determine the angular scattering functions, there is no explanation or discussion as to how shattered artefacts were removed from the analysis. Please could you insert this, otherwise, we may be led to believe that those functions could be more pertinent to shattered ice and so will provide low asymmetry parameter estimates. The Referee is correct that the influence of the shattering artefacts to the PHIPS and PN measurements are not adequately discussed in Section 2.2. Since PHIPS performs particle-by-particle measurements, it is possible to detect shattering events by investigating the particle inter-arrival times. The analysis of the particle inter-arrival times revealed two modes - one mode of short inter arrival times corresponding to shattering events and one mode of longer inter arrival times corresponding to real particle events. These two modes can be separated with a threshold of approximately 1 ms. We have removed all the angular scattering functions identified as shattered events from the analysis.

The analysis of the PN data, including shattering artefacts, is discussed in the original publications cited in this manuscript and in previous studies. For example, the effects of shattering artefacts to the PN measurements are discussed in the Appendix B of Mioche et al. (2017). The authors stated that although it is not possible to avoid or estimate the shattering effects in the PN signal, it can be estimated that the shattering artefacts are within the measurement uncertainty of the PN (25 % on the extinction coefficient).

Two sentences discussing the shattering effects were added to the Section 2.2 after discussion of both instruments:

PHIPS: *“Before analysis, particles corresponding to shattering events were removed by calculating particle inter-arrival times and removing particle pairs with inter-arrival times <1ms.”*

PN: *“It is not possible to correct the PN data for shattering artefacts but it has been estimated that possible shattering artefacts contribute less than 25% to the total extinction signal (Mioche et al., 2017).”*

14. Section 2.4, perhaps save space by compiling the list of campaigns into a table? This improves readability.

Section 2.4 does not only give a list of the campaigns but also discusses the definition “ice cloud” in each of the campaigns (i.e. which cloud types were included in the analysis). The discussion presented in Sect. 2.4 is relevant for understanding the results, since different cloud systems were sampled in different campaigns. Furthermore, this section gives a description, how droplets were excluded from the dataset. For these reasons, we think Sect. 2.4 is important and cannot be reduced as a table.

15. There are many campaigns dating back to before 2010, how did the authors make sure that the PSDs were treated consistently into one database from the variety of differing microphysical probes?

This manuscript reports measurements from three different microphysical probes: the Small Ice Detector 3 (SID-3), the Particle Habit Imaging and Polar Scattering (PHIPS) probe and the Polar Nephelometer (PN). All the SID-3 and PHIPS data from each of the field campaigns are analyzed using the procedures described in the Sections 2.1 and 2.2. Also, the analysis methods of the PN probe have not been modified since published in Gayet et al. 1997.

16. Page 5, line 23, suggest replace “to” with “for” . . . the analysis. . .

We corrected this.

17. Section 2.5, please add a description of the current ice optical parameterization used in ECHAM-HAM. It is often referred to but unknown as to what it actually is.

The current ice optical parameterization in the ECHAM-HAM is calculated with Mie-theory but the asymmetry parameters are scaled down to be more reliable for aspherical ice particles. We added this description of the current optical parameterization to Sect. 4, where the ECHAM-HAM model is discussed.

18. Page 7, line 6, suggest insert the word “to”. . . a change. . .

We corrected this.

19. Page 7, line 10, comma after aggregates?

We added a comma.

20. Page 8, there are a whole list of studies that predate 2010 in showing that flat featureless phase functions best represent angular short-wave measurements obtained from above ice cloud such as Doutriaux-Boucher et al., (2000)[ <https://agupubs.onlinelibrary.wiley.com/doi/abs/10.1029/1999GL010870> ], Labonnote et al. (2001)[ <https://agupubs.onlinelibrary.wiley.com/doi/abs/10.1029/2000JD900642> ]. A more recent paper by Letu et al. (2016) [<https://www.atmos-chem-phys.net/16/12287/2016/>] uses comprehensive PARASOL short-wave reflectance data to show the same.

We extended the references as suggested.

21. Page 8, line 16, Again, there are many papers that predate 2013, please cite a representative sample.

We extended the references by citing Macke et al. (1996), Yang and Liou (1998), Liou et al. (2000), Baum et al. (2010), Baum et al. (2011), Baran (2012), Diedenhoven et al. (2012). We also added e.g. before the references to illustrate that the cited references are a subsample of literature.

22. Page 9, line 5, typo “sdiscussed”.

We corrected this.

Figures:

Fig. 1 penale-> panel.

We corrected this.

Fig. 2 difficult to distinguish purple from red, suggest changing purple to green.

We changed the purse trajectories to green and modified the colours in Fig. 3 accordingly.

Table 2. Please also insert the percentage of the total particle population rejected owing to shattering.

We have added a new column to the table showing the percentage of ice particles rejected owing to shattering.

## References

Gayet, J.-F., Crépel, O., Fournol, J., and Oshchepkov, S.: A new airborne polar Nephelometer for the measurements of optical and micro- physical cloud properties. Part I: Theoretical design, *Annales Geophysicae*, 15, 451–459, 1997.

Liu C., R. L., Panetta, P., Yang, 2013: The effects of surface roughness on the scattering properties with sizes from the Rayleigh to the geometric-optics regimes. *J. Quant. Spectrosc. Radiat. Transfer.*, 129:169-185.

Mioche, Guillaume, et al. "Vertical distribution of microphysical properties of Arctic springtime low-level mixed-phase clouds over the Greenland and Norwegian seas." *Atmospheric Chemistry and Physics* 17 (2017): 12845-12869.

## Authors' Response to Anonymous Referee #2 Comments

The authors would like to thank the anonymous Referee for her/his helpful comments. Please find below a detailed point-by-point replies to each comment. Referee's comments are in blue and authors' replies in black.

In this article, ice particle complexity was derived from field campaigns spread over the globe, and it was further compared to chamber study. Angular light scattering functions from measurements were compared to Ping Yang's models, and it was concluded that roughened column aggregates model is the best representative of measurements. The new asymmetric factor derived from roughened column aggregates was explored in changing cloud radiative effects using a climate model. Overall, this article is well constructed and novel. Particularly, comparison of phase function between measurement and theoretical model will benefit other research areas such as model parameterization or remote sensing. My general comments: 1) explain how to obtain SWCRE from ECHAM model; 2) indicate how large biases of phase function exist between smooth and roughened particles.

We thank the Referee for her/his encouraging comments. To address the general comment (1) we have added a detailed description on how SWCRE was obtained using the ECHAM model. Please see the answer to the specific comments below for more details.

In the general comment (2) the Referee asks to address the differences between the phase functions and asymmetry factors of smooth and severely roughened particles. For the database used in this manuscript, this difference is discussed in the original study of Yang et al. (2013). In Fig. 13 of their paper a comparison is shown of phase functions and asymmetry factors for smooth and roughened particles. The phase functions of smooth particles show minima and maxima peaks at certain angles whereas as the roughness is increased, these peaks are more smoothed out (please also see the answer to the specific comment below). Also, the intensity at the sideward angles is the highest for the roughest particles, which leads to lowering of the asymmetry factor as seen in the lower panels of Fig. 13.

These biases between the phase functions of smooth and roughened particles are discussed in several occasions in this manuscript (please see answers below) and in the cited research (e.g. in Yi et al. (2013)). We think that the given discussion together with the references give the reader a good overview of the effects of roughness on the phase function and on the asymmetry factor.

Suggestion is to accept after a minor revision.

### Specific comments:

#### Page 2

Lines 15-17: 'reduce the SWCRE by 1-2 W m<sup>-2</sup>' is confusing. It reads like that the magnitude of SWCRE is reduced, i.e. SW cooling is reduced by lowering g. This is conflicted with your conclusion. Please double check Yi et al. 2013 and make it clear.

We agree that the wording online 15-17 is confusing, so we reformatted the sentence as: "*Yi et al. (2013) showed that by assuming severely roughened ice crystals and, thus, lowering the cloud short wave (SW) asymmetry factors between 0.01 and 0.035, can cause additional SW cooling by 1-2 W m<sup>-2</sup>.*"

Line 29: Please indicate what are 'two instruments'.

We added the names of the two instruments: "*The observations of the ice crystal mesoscopic complexity are linked with measurements of the ice particle angular light scattering function at various geographical locations in the southern and northern hemisphere performed with two polar nephelometers, the Particle Habit Imaging and Polar Scattering (PHIPS) probe and the Polar Nephelometer (PN).*"



Figure 1” upper panel->upper panel ; In lower panel, some scales are not clear.

We corrected this and increased the font of the scales in the lower panel.

Page 5 line 29: ‘In these campaigns’, do you mean all arctic campaigns ? Are there mixed phase clouds in SOCRATES campaign or midlatitude campaigns such as ARISTO 2017 and CONCERT with relatively high temperatures?

Yes, we mean all arctic campaigns. We changed in the text “*In these campaigns*” to “*In the arctic campaigns*”.

We measured mixed-phase clouds in the SOCRATES campaign but in the midlatitude campaigns only measurements in fully glaciated clouds are included. To make this more clear we added the term “mixed-phase” on line 1 (page 6).

Page 6, section 2.5: Could you explain clearly how do you obtain SWCRE from ECHAM? Is it a parameter output from ECHAM, or do you run a radiative transfer model using ice clouds output from ECHAM?

We have added a detailed description of how SWCRE was obtained from the ECHAM model in the chapter 2.5.

*“The ECHAM-HAM model is used to calculate the SWCRE of the ice clouds, which is computed online by calling the radiation subroutine twice. The first call is with clouds (all-sky) and the second call is without clouds (clear-sky) in the atmosphere. The first call uses the standard model parameterization for the short wave asymmetry factors of ice clouds. The radiative fluxes from this call to the radiation subroutine are used to advance the model simulations. The cloud radiative effects are computed as the difference between the all-sky minus the clear-sky fluxes. To estimate the change in SWCRE by changing the short wave asymmetry factors of ice clouds an additional (third) call to the radiation subroutine is conducted. The additional (diagnostic) call to the radiation subroutine is identical to the first call except for using the new parameterization for the short wave asymmetry factors of ice clouds. The radiative fluxes from this additional call are only diagnostic. The SWCRE using the new parameterization for the short wave asymmetry factors of ice clouds is computed from the difference in SW radiative flux at the top of the atmosphere from the additional call and the cloud-free SW radiative flux at the top of the atmosphere.”*

Page 8

Line 20: ‘For generation of the theoretical phase functions.....’, do you mean that the phase function here is not for only one particle, instead for integration of a series of particles like bulk property?

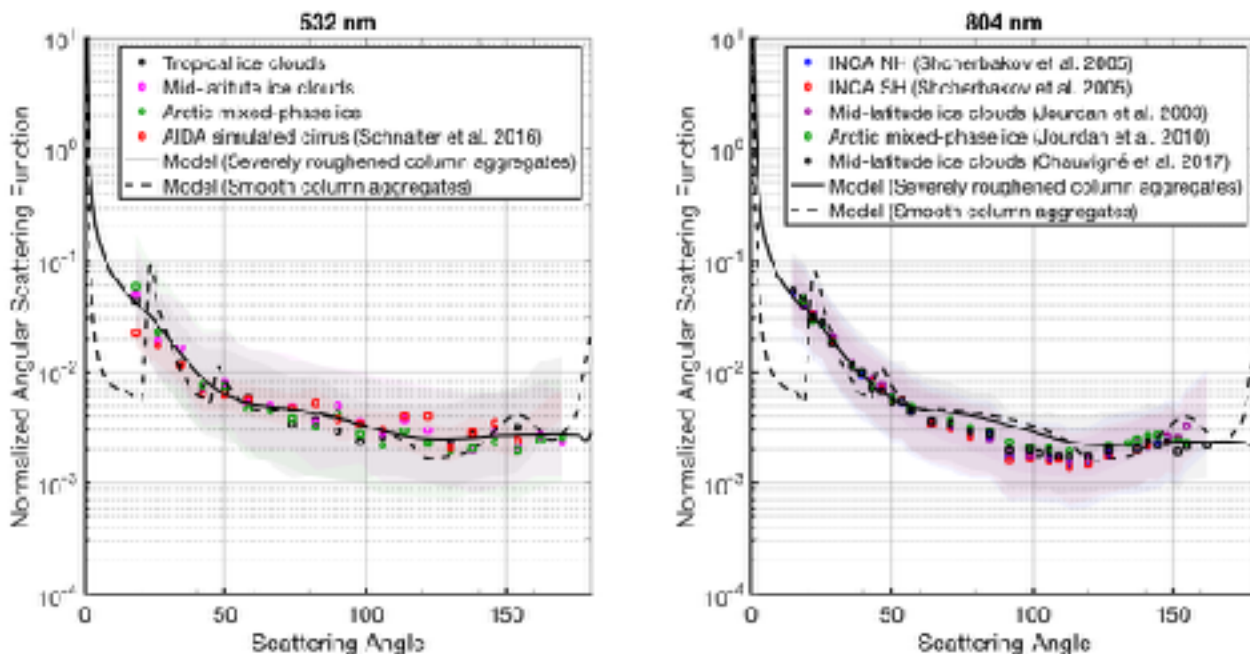
The theoretical phase functions are calculated for orientation averaged particles that are integrated over a size distribution - similar to the measurements that are also averaged over a particle population. To make this more clear we modified the caption of Fig. 5: “*A comparison of the measured angular light scattering functions at 532 nm (data from first panel of Fig. 4) and theoretical phase functions for different habits calculated using the database of Yang et al. (2013) and assuming a size distribution as measured during the ACRIDICON-CHUVA campaign. All calculations...*”.

Figure 4 and Figure 5: are the measured ‘angular light scattering functions’ the same in both figures? If yes, please indicate. Also, roughened particles are used here for comparison because studies indicate that they perform well in many applications. How would the smooth particle model curve look like if they are overplotted in Figures 4 and 5?

The data in the first panel of Fig. 4 is the same as seen in Fig. 5. We indicated this in the Fig. 5 caption: “*A comparison of the measured angular light scattering functions at 532 nm (data from first panel of Fig. 4)...*”.

A comparison of phase functions of smooth and roughened particles from the used database are shown in Fig. 13 of Yang et al. (2013). This figure shows that smooth particles have distinct features in the phase function that are not well represented by our measurements. Overplotting the phase functions of smooth particles to Figs. 4 and 5 would make the figures too full and could

distract the reader from evaluating the difference between the measurements and the different severely roughened models (please see figure below). We think that the comparison between smooth and roughened particles is adequately discussed and shown in the cited literature so that it is not needed to show the smooth phase functions in Figs. 4 and 5. Further, the differences in the phase functions of smooth and roughened particles are described in the Introduction and in Sect. 4.



Page 10

Line 8: ‘ the global mean change in the SWCRE is  $-1.12 \text{ W m}^{-2}$ ’, please indicate that more cooling is brought in using new g parameterization.

We have modified the first sentence of paragraph 4.2 to: “*The change in the global SWCRE after applying the new parameterization to all ice clouds (cirrus and mixed-phase) is shown in Fig. 8. The global mean change in the SWCRE is  $-1.12 \text{ W m}^{-2}$ , but...*”

Line 9: ‘ the change in global SWCRE is small compared to ....’, yes, it is right. However, based on Section 2.5, SWCRE is for ice clouds only. Is the change significant relative to your simulated SWCRE with new and old parameterizations? How about compare to SWCRE by ice clouds from [Gasparini and Lohmann, 2016] and [Hong et al., 2016] where show ice cloud radiative effect using ECHAM-HAM model and from observations?

The change in the SWCRE take into account all ice clouds (cirrus and mixed-phase). To make this more clear we modified the sentence on page 10 line 7 (old manuscript) the following: “*The change in the global SWCRE after applying the new parameterization to all ice clouds (cirrus and mixed-phase) is shown in...*”.

We can directly compare our estimated change in the SWCRE to the one SWCRE calculated by Hong et al. (2016) but not to the one SWCRE calculated by Gasparini and Lohmann (2016) since this was calculated for cirrus clouds only. We have calculated the change in the SWCRE also only for cirrus clouds but this estimation was not shown in the manuscript. We added this information to the revised manuscript and modified the discussion the following: “*If the new parameterization is applied only for cirrus clouds, the mean change in the SWCRE is slightly lower,  $-1.00 \text{ W m}^{-2}$ . Therefore, the change in the asymmetry factor mostly affects the cirrus SWCRE and, also, the largest effect is found in the tropical regions where also the cirrus occurrence is the highest (e.g. Sassen et al., 2008). Even though the change in the global SWCRE is small compared to the*

global mean SWCRE of all clouds of about  $-50 \text{ W m}^{-2}$  (Boucher et al., 2013) or to the global mean SWCRE of ice clouds of about  $(-16.7 \pm 1.7 \text{ W m}^{-2})$  (Hong et al., 2016) it is one fourth of the global mean cirrus SWCRE of  $-4 \text{ W m}^{-2}$  (Gasparini and Lohmann, 2016) and comparable to the total direct radiative effect of aerosols  $(-2.1 \pm 0.7 \text{ W m}^{-2})$  (Lacagnina et al., 2017)".

Line 11: 'the decrease in SWCRE...', please indicate cooling is enhanced.

We replaced the term "*the decrease in SWCRE*" with "*The enhanced SW cooling*".

'cirrus CRE', please explain what ice clouds have been used for CRE studied? Thin cirrus only?

The term "cirrus CRE" here refers to the CRE by cold ( $< -40^\circ\text{C}$ ) ice clouds. Here, the term "cirrus CRE" is used to generally refer to all cirrus clouds.

## References

Gasparini, B., and U. Lohmann (2016), Why cirrus cloud seeding cannot substantially cool the planet, *J. Geophys. Res. Atmos.*, 1–17, doi:10.1002/2015JD024666.

Hong, Y., G. Liu, and J.-L. F. Li (2016), Assessing the Radiative Effects of Global Ice Clouds Based on CloudSat and CALIPSO Measurements, *J. Clim.*, (2011), In press, doi:10.1175/JCLI-D-15-0799.1.

## References

Yang, P., Bi, L., Baum, B. A., Liou, K.-N., Kattawar, G. W., Mishchenko, M. I., and Cole, B.: Spectrally consistent scattering, absorption, and polarization properties of atmospheric ice crystals at wavelengths from 0.2 to 100  $\mu\text{m}$ , *Journal of the Atmospheric Sciences*, 70, 330–347, 2013.

Yi, B., Yang, P., Baum, B. A., L'Ecuyer, T., Oreopoulos, L., Mlawer, E. J., Heymsfield, A. J., and Liou, K.: Influence of Ice Particle Surface Roughening on the Global Cloud Radiative Effect, *Journal of the Atmospheric Sciences*, 70, <https://doi.org/10.1175/JAS-D-13-020.1>, 2013.

## Authors' Response to Anonymous Referee #3 Comments

The authors would like to thank the anonymous Referee for her/his helpful comments. Please find below a detailed point-by-point replies to each comment. Referee's comments are in blue and authors' replies in black.

This paper describes the submicron scale complexity of individual ice crystals derived from airborne measurements and cloud chamber experiments. The authors assess that a new radiation parameterization for global climate models considering the higher roughness of ice crystals reveals a lower SWCRE. I find the paper very well written, logically organized, and the figures and tables are appropriate. I recommend the paper to be published with minor revision.

We thank the anonymous Referee for this very encouraging general comment. Below we address the suggested minor revisions.

Special comments:

1. Page 2, Line 30/31: "In two cases the crystal complexity measurements and the angular light scattering measurements were conducted on the same ice particle population." I did not get where you use this coupled information later. Or is there any advantage at all having the measurements on the same ice particle population?

One of the main conclusions in this manuscript is that the high degree of ice crystal complexity is the reason why a similar angular scattering function is measured at different geographical locations. Two cases, where the two measurements ice crystal complexity and angular light scattering measurements) were performed on the same particle population, helps justify this conclusion.

2. Page 3, Line 22/23: Why is there more shattering in mixed-phase clouds?

Shattering is enhanced by the presence of large ice crystals and ice crystals with certain habits, such as bullet rosettes or large aggregates. In mixed-phase clouds, there tend to be more precipitation-sized ice crystals and rimed (aggregated) ice crystals. Jackson et al. (2014) showed that at temperatures  $> -8^{\circ}\text{C}$  more shattering is present than in colder temperatures due to the presence of rimed ice crystals. These observations would explain the higher fraction of shattering in mixed-phase clouds since most of these measurements happened at temperatures warmer than  $-8^{\circ}\text{C}$ .

We modified the sentence on page 3, line 22/23 the following: "*In mixed- phase clouds a higher fraction of measured 2-D scattering patterns, between 7.5% and 19%, were excluded from analysis. The higher fraction of shattering in mixed-phase clouds can be explained by the presence of rimed particles (Jackson et al., 2014)*".

3. Page 8, Line 20: Why is the size distribution from the ACRIDICON-CHUVA campaign representative?

The size distribution from the ACRIDICON-CHUVA campaign is measured for the same particles whose angular scattering functions are shown, i.e. the size distribution corresponds to the scattering information. It was also investigated how sensitive the retrieved angular scattering function is to the assumed size distribution and it was found to be insensitive to small changes in the median diameter. This is explained in the text at page 8 lines 22 and 23 (old manuscript version). Therefore, the exact size distribution is not crucial for finding the best fit.

4. Page 10, Line 8: Why are these regional differences in the change of SWCRE? Why is the signal mainly in the tropics?

The regional differences are linked with the cirrus occurrence. The cirrus occurrence is the highest in the tropics which, consequently, leads to the largest change in the SWCRE. We added a sentence in the chapter 4.2 to explain the regional differences: "*The largest effect is found in the tropical regions where also the cirrus occurrence is the highest (e.g. Sassen et al., 2008)*".

5. Page 11, Line 4: Before you could investigate the role in a warmer climate, you need to know if there are changes of the submicron scale complexity in a warmer climate. Do you expect them? This is a difficult question to answer as long as we do not really understand the origin of submicron scale complexity in ice crystals. The only evidence we have is that abundance of heterogeneous ice nucleating particles (INPs) might decrease the supersaturation needed to nucleate the ice and, therefore, could lead to decrease in ice crystal mesoscopic complexity. However, increase in INPs also changes the cloud optical depth, which leads to another forcing.

With the statement on page 11 line 4 we wanted to motivate studies to investigate how cirrus radiative forcing would change if mesoscopic complexity is included in the projections versus if assuming the standard parameterisation.

#### Technical corrections:

1. Page 3, Line 3; Page 5, Line 2; Page 7, Line 8: “sub-micron”. Mostly you write “submicron”, hyphenless.

We changed the term “sub-micron complexity” to “mesoscopic complexity” in the entire text. The reason for this was a critique towards presenting a new term to the field whereas the term “mesoscopic complexity” is already established.

#### References

Jackson, R. C., McFarquhar, G. M., Stith, J., Beals, M., Shaw, R. A., Jensen, J., Fugal, J., and Korolev, A.: An assessment of the impact of antishattering tips and artifact removal techniques on cloud ice size distributions measured by the 2D cloud probe, *Journal of Atmospheric and Oceanic Technology*, 31, 2567–2590, 2014.

## Authors' Response to Interactive Comment by Z Ulanowski

The authors appreciate the Interactive Comments made by Z Ulanowski. Below we provide our answers to the raised issues. The Interactive Comments are in blue and authors' replies in black.

This extensive study investigates a very important area concerning the radiative impact of atmospheric ice. It could make an important contribution to this subject. However, several conclusions being made are too strong in my view and should be qualified. There is also one large flaw that should be addressed to increase the value of the study.

We thank Z Ulanowski for acknowledging the importance of this study and address his comments below.

4.2 p.10. My main point is a significant weakness of this study, the omission of long-wave (LW) effects of cirrus. To illustrate the importance of this shortcoming, the cirrus radiative effect difference found here is dominated by changes in the Tropical Warm Pool (TWP) and Maritime Continent. Yet in this region the net radiative influence of cirrus is determined largely by the longwave, with difference from even the zonal average of the order of many tens of  $W/m^2$  (e.g. Xu and Guan, 2017; NOAA/ESRL), in contrast to the `_peak_ SW` value of about  $8W/m^2$  reported here. So potentially not just the magnitude but even the sign of the postulated effect could change. Hence the LW effect should be taken into account. The severely roughened hexagonal aggregate model that is adopted by the authors includes IR properties. Why were they not included to obtain the net radiative effect? Was the longwave parameterization done but the effects are not shown - why, it should be easy to do? Or was the parameterization not applied - which makes the model internally inconsistent? If this result is being kept "for later", I would strongly advise against it - salami-slicing climate science is a risky undertaking, e.g. the longwave cloud feedback is reported to be positive, mostly due to tropical cirrus (Zelinka and Hartmann, 2010), potentially negating the main conclusion from the work.

In this study we only discuss the effect of ice crystal complexity to the SWCRE and omitting the LW effect will not in any way change the conclusion of this work. There are two reasons why we do not discuss the LW effect. First, the focus of this study is the effect of ice crystal complexity on the ice cloud asymmetry factor. In the ECHAM-HAM model the ice particle asymmetry factors are only considered for calculation of the SW effect and are not included in the calculations of the LW effect. This is due to the fact that the LW effect is less sensitive to the ice crystal morphology than the SW effect. For example, Yi et al. (2013) showed that changing the ice crystals from smooth to complex will not significantly affect the LWCRE.

Secondly, our optical measurements are in the SW region and, therefore, we can only make conclusion of the SW asymmetry factors. We agree that optical measurements in the LW region would be of interest to validate LW parameterizations in the future. Furthermore, we think that the term "salami-slicing" is more than misplaced with regard to this work, which - in our opinion - represents one of the most comprehensive studies on ice crystal complexity and its influence on the cloud radiative forcing. The experimental data used here are from dedicated cloud chamber simulation runs as well as from the field, gathered in a dozen of aircraft projects around the globe. Further, the data are used to construct a new, more realistic parameterization of the asymmetry factor to be used in climate models - a scientific span that is not common in the field.

This brings me to a related point: the authors make strong statements about the radiative impact, with the largest impact being demonstrated in the TWP/MC region. Yet no in situ data from this region is provided, and very little data from the tropics altogether. What there is, refers to Amazonia, where modelling indicates very weak impact.

The data presented in this study covers all the geographical areas where the KIT SID-3 and the PHIPS instruments have been flown and a large amount of the campaigns where PN measurements were available. We agree that the TWP/MC region (where these instruments have not yet flown) is highly important for the cirrus cloud radiative impact. We hope that in future more field campaigns will be focused on this area, where this study demonstrates the largest SW impact.

Some smaller points follow.

Introduction p.2 and section 2.1 p.3. I find it surprising that the authors do not properly acknowledge that SID3, the core instrument in this work, and long-term assistance with the hardware, software and data analysis techniques were provided to KIT by the team at University of Hertfordshire.

The SID-3 instrument was developed by the University of Hertfordshire and a version of the instrument was purchased by KIT in 2008. It is true that many collaborative efforts between KIT and Hertfordshire has taken place to improve the hardware, software and data analysis methods to the current status and we believe that these collaborative efforts are correctly documented in the corresponding literature. The instrument itself is cited through the original Hertfordshire publication of Kaye et al. (2008). The University of Hertfordshire was involved in the first field deployment of the instrument in the MACPEX campaign, which is acknowledged by co-authorship in the Järvinen et al. (2016) and Schmitt et al. (2016b) publications. The SID-3 scattering pattern analysis methods for atmospheric ice particles were also developed in close collaboration between KIT and University of Hertfordshire by conducting at least five joint AIDA cloud simulation campaigns. This effort is acknowledged in the original work describing the use of the complexity parameter,  $k_e$ , as a complexity measure (Schnaiter et al., 2016), where the University of Hertfordshire (Z Ulanowski) is listed as co-author.

2.1 p.3. Likewise, the method for determining ice crystal roughness using pattern texture analysis (including GLCM) was developed by the Hertfordshire group (Ulanowski et al., 2010, 2014). This should be acknowledged too.

Analysing scattering patterns to retrieve information on surface roughness has been previously used in industrial applications for surface quality control (e.g. Lu et al., 2006) but it is true that the Hertfordshire group was the first to use this technique for ice crystal surface roughness.

Therefore, we have added the citation to Ulanowski et al., 2010, 2014 to the following sentence:

*“The crystal complexity is quantified from the 2-D scattering patterns using a grey-level co-occurrence matrix (GLCM) method (Lu et al., 2006). This method was developed for industrial quality control of surface treatment processes but was later adapted for analysis of complexity features of three-dimensional ice particles (Ulanowski et al., 2010, 2014; Schnaiter et al., 2016).”*

3.2 p.7. "enhanced submicron scale complexity of homogeneously formed ice crystals [...] and can be explained by an increased stacking disorder of homogeneously nucleated ice crystals" Firstly, it would be difficult to associate in situ measurements with the homogeneous mode of nucleation in such categorical fashion. The second part of this statement is extremely simplistic too, no proof of a general connection of complexity with stacking disorder exists yet, even in the lab let alone the atmosphere. While stacking-disordered ice has been produced in the supercooled water freezing experiments of Malkin et al. (2012), heterogeneous ice nucleation is equally important and there can be other reasons why roughness arises (Chou et al., 2018).

We refer to the in situ measurements that were presented in Ulanowski et al. (2014). The authors argued that in situ observations in a mid-latitudes cirrus showed differences in the ice crystal complexity based on the airmass origin: *“polluted airflow showed significantly lower roughness for all measures apart from kurtosis. We speculate that this was due to higher concentration of inhomogeneous ice nuclei (IN) in the last case”*. Of course it is difficult to investigate the origin of ice crystal complexity based on in situ measurements, especially if the ice particle history is unknown. Therefore, such laboratory studies will be valuable to interpreted in situ field results.

For the second point, we agree that our knowledge of formation of surface roughness in a single crystal is still highly unknown. Therefore, we modified the sentence as: *“can be partly explained by...”*.

3.2. p7. While cyclic growth has been shown to contribute to increased ice roughness (Chou et al., 2018) the SEM experiments that are cited (Magee et al., 2014) are thought to have limited relevance to ice behaviour at tropospheric conditions, as growth in the near-vacuum of a SEM takes place under kinetically-limited, not diffusion-limited conditions typical of the troposphere (Kiselev, 2014; Chou et al., 2018).

We agree that discussing the results of SEM experiments in atmospheric context is challenging due to the near-vacuum pressure conditions experienced by the ice crystals. Therefore, it is important to have proof such results in atmospheric conditions as shown in Chou et al. (2018). We have added this reference to the sentence together with the Magee et al. (2014) reference.

#### References

- Chou C., Voigtländer J., Ulanowski Z., Herenz P., Bielick H., Clauss T., Niedermeier D., Hartmann S., Ritter G., Stratmann F.: Ice crystals roughness during depositional growth and sublimation, *Atm. Chem. Phys.*, doi:10.5194/acp-2018-254, in review, 2018.
- Kiselev, A.: Interactive comment on "Mesoscopic surface roughness of ice crystals pervasive across a wide range of ice crystal conditions" by N. B. Magee et al., *Atmos. Chem. Phys. Discuss.*, 14, C4758–C4763, <http://www.atmos-chem-phys-discuss.net/14/C4758/2014/>, 2014.
- Malkin, T. L., Murray, B. J., Brukhno, A. V., Anwar, J., and Salzmann, C. G.: Structure of ice crystallized from supercooled water, *Proceedings of the National Academy of Sciences*, 109, 1041–1045, 2012.
- NOAA/ESRL <http://www.esrl.noaa.gov/psd/>
- Ulanowski Z., P.H. Kaye, E. Hirst & R.S. Greenaway: Light scattering by ice particles in the Earth's atmosphere and related laboratory measurements, In: *Proc. 12th Int. Conf. Electromagnetic & Light Scatt.*, Helsinki, 294-297, 2010.
- Zelinka, M. D., and D. L. Hartmann: Why is longwave cloud feedback positive?, *J. Geophys. Res.*, 115, D16117, doi: 10.1029/2010JD013817, 2010.
- Xu, Q. and Guan, Z.: Interannual variability of summertime outgoing longwave radiation over the Maritime Continent in relation to East Asian summer monsoon anomalies, *J. Meteorological Research*, 31, 665-677, 2017.

#### References

- Järvinen, E., Schnaiter, M., Mioche, G., Jourdan, O., Shcherbakov, V. N., Costa, A., Afchine, A., Krämer, M., Heidelberg, F., Jurkat, T., Voigt, C., Schlager, H., Nichman, L., Gallagher, M., Hirst, E., Schmitt, C., Bansemer, A., Heymsfield, A., Lawson, P., Tricoli, U., Pfeilsticker, K., Vochezer, P., Möhler, O., and Leisner, T.: Quasi-Spherical Ice in Convective Clouds, *Journal of the Atmospheric Sciences*, 73, 3885–3910, <https://doi.org/10.1175/JAS-D-15-0365.1>, 2016.
- Kaye, P. H., Hirst, E., Greenaway, R. S., Ulanowski, Z., Hesse, E., DeMott, P. J., Saunders, C., and Connolly, P.: Classifying atmospheric ice crystals by spatial light scattering, *Opt. Lett.*, 33, 1545–1547, 2008.
- Lu, R.-S., Tian, G.-Y., Gledhill, D., and Ward, S.: Grinding surface roughness measurement based on the co-occurrence matrix of speckle pattern texture, *Appl. Opt.*, 45, 8839–8847, 2006.
- Schmitt, C. G., Schnaiter, M., Heymsfield, A. J., Yang, P., Hirst, E., and Bansemer, A.: The microphysical properties of small ice particles measured by the Small Ice Detector-3 probe during the MACPEX field campaign, *Journal of the Atmospheric Sciences*, 2016b.



# Additional Global Climate Cooling by Clouds due to Ice Crystal Complexity

Emma Järvinen<sup>1</sup>, Olivier Jourdan<sup>2</sup>, David Neubauer<sup>3</sup>, Bin Yao<sup>4</sup>, Chao Liu<sup>4</sup>, Meinrat O. Andreae<sup>5,6</sup>, Ulrike Lohmann<sup>3</sup>, Manfred Wendisch<sup>7</sup>, Greg M. McFarquhar<sup>8,9</sup>, Thomas Leisner<sup>1</sup>, and Martin Schnaiter<sup>1</sup>

<sup>1</sup>Karlsruhe Institute of Technology, Institute of Meteorology and Climate Research, Karlsruhe, Germany

<sup>2</sup>Laboratoire de Météorologie Physique, Université Clermont Auvergne, OPGC, UMR/CNRS 6016, Clermont-Ferrand, France

<sup>3</sup>Institute of Atmospheric and Climate Science, ETH Zürich, Zürich, Switzerland

<sup>4</sup>Collaborative Innovation Center on Forecast and Evaluation of Meteorological Disasters, Nanjing University of Information Science and Technology, Nanjing 210044, China

<sup>5</sup>Biogeochemistry Department, Max Planck Institute for Chemistry, Mainz, Germany

<sup>6</sup>Scripps Institution of Oceanography, University of California San Diego, La Jolla, California, USA

<sup>7</sup>Leipzig Institute for Meteorology, University of Leipzig, Leipzig, Germany

<sup>8</sup>Cooperative Institute for Mesoscale Meteorological Studies, University of Oklahoma, Norman, OK

<sup>9</sup>School of Meteorology, University of Oklahoma, Norman, OK

**Correspondence:** Emma Järvinen (jarvinen@ucar.edu)

**Abstract.** Ice crystal submicron structures have a large impact on the optical properties of cirrus clouds and consequently on their radiative effect. Although there is growing evidence that atmospheric ice crystals are rarely pristine, direct in-situ-in situ observations of the degree of ice crystal complexity are largely missing. Here we show a comprehensive in-situ-in situ dataset of ice crystal complexity coupled with measurements of the cloud asymmetry factor collected at diverse geographical-angular scattering functions collected during a number of observational, airborne campaigns at diverse geographical locations. Our results demonstrate that an overwhelming fraction (between 61 and 81%) of atmospheric ice crystals sampled in the different regions sampled contain submicron contain mesoscopic deformations and, as a consequence, a low asymmetry factor of 0.75 similar flat and featureless angular scattering function is observed. The measured cloud angular light scattering functions were parameterized in terms A comparison between the measurements and a database of optical particle properties showed that severely roughened hexagonal aggregates optimally represents the measurements in the observed angular range. Based on this optical model, a new parameterization of the cloud bulk asymmetry factor and was introduced and its effects were tested in a global climate model. The modelling results suggest that due to ice crystal complexity, ice-ice-containing clouds can induce an additional short wave cooling effect of  $-1.12 \text{ W m}^{-2}$  on the top-of-the atmosphere radiative budget that has not yet been considered.

## 15 1 Introduction

Atmospheric ice crystals exhibit considerable variability in growth habits (Heymsfield and Platt, 1984; Korolev et al., 1999; Lawson et al., 2006), which makes their representation in global and regional climate and weather-numerical weather prediction

models challenging. Moreover, laboratory observations and satellite retrievals have shown that ~~submicron-structures-of-the-ice crystals~~ice crystal mesoscopic structures, such as surface roughness or other crystal deformations, which have been observed in various environmental conditions (~~Diedenhoven et al., 2012; Neshyba et al., 2013; Cole et al., 2014; Magee et al., 2014~~)(Ulanowski et al., 2014) can further complicate their ~~representation~~realistic representation. Ice crystal surface roughness was added as a new variable to 5 models of ice particle optical properties (~~Yang et al., 2008; Baum et al., 2010; Platnick et al., 2017~~)(e.g. Macke et al., 1996; Yang and Liou, 2007). Later, it was found that ice crystal parameterizations implementing roughened surfaces represent the measured optical properties, and especially the polarization effects of atmospheric ice clouds, more accurately than parameterizations based on a mixture of pristine ice crystals (~~Um and McFarquhar, 2007; Jourdan et al., 2010; Liu et al., 2014b; Yi et al., 2016; Tang et al., 2017~~)(Baran and McFarquhar, 2010). Currently, severely roughened aggregated ice crystals are assumed in remote sensing retrieval algorithms (Platnick et al., 10 2017), and it has been suggested to include ~~severely-roughened-this type of~~ ice crystals in the radiative transfer algorithms of general circulation models (Yi et al., 2016). However, the observational justification of this approach is still lacking ~~because sufficient observational~~, mainly because sufficient evidence of frequent occurrence of roughened ice crystals in different types of ice-containing clouds has not been ~~provided~~obtained yet.

Surface roughness changes the ice crystal single scattering properties significantly. Light scattering calculations have shown 15 that, compared to pristine ice crystals, ice particles with roughened surfaces produce flat and featureless angular ~~light~~-scattering functions that ~~have a significantly higher~~reveal a significantly elevated backward scattering and, therefore, a lower asymmetry factor compared to their smooth counterparts (Yang and Liou, 1998; Ulanowski et al., 2006; Baum et al., 2011; Yi et al., 2016). ~~In-situ~~In situ observations at several geographical locations have given indications of low asymmetry factors in ice clouds in the range of 0.74 to 0.79 (Gerber et al., 2000; Gayet et al., 2006; Febvre et al., 2009; Jourdan et al., 2010). However, 20 without simultaneous measurements of the ice particle surface roughness, it remains unclear if the measured low asymmetry factors of natural ice clouds are induced by this feature. In general, more measurements of the cloud asymmetry factor are needed, since a small change in the asymmetry factor can have significant consequences for the short wave cloud radiative effect (SWCRE). Yi et al. (2013) showed that ~~by~~ assuming severely roughened ice crystals and, thus, lowering the cloud short wave (SW) asymmetry factors by values between 0.01 and 0.035, can ~~reduce the SWCRE by~~cause an additional SW cooling 25 of 1-2 W m<sup>-2</sup> at the top-of-the atmosphere.

Recent developments in airborne ~~in-situ~~in situ measurement techniques have enabled ~~a direct way to to~~directly measure ice crystal complexity at ~~submicron-seales~~mesoscopic scales (here defined as structures in a scale between 100 nm to 10 μm), which had previously been too small to be resolved from cloud particle imager measurements. The Small Ice Detector Mark 3 (SID-3) (Kaye et al., 2008) records the spatial distribution of ~~the~~coherent laser light scattered by individual ice ~~partieles~~crystals 30 (examples of scattering patterns ~~seen-are shown~~ in Fig. 1). The image texture of the resulting ~~single-partiele~~single-particle scattering patterns can be analysed to retrieve ~~a~~the so-called complexity parameter,  $k_e$ , that has proven to be a suitable proxy for the actual ice crystal ~~submicron-mesoscopic~~mesoscopic complexity (Schnaiter et al., 2016). In this context, ~~the submicron-scale ice crystal-mesoscopic~~mesoscopic complexity comprises all crystal deformations (e.g., surface roughness, hollowness, and air inclusions), which result in the formation of speckles in the coherent light scattering by these particles. Since the SID-3 instrument does

not discriminate between mesoscopic complexity and surface roughness, for the remainder of this paper the term *ice crystal mesoscopic complexity* is used instead of the more established term *ice crystal surface roughness*.

In this paper, this Here, the complexity analysis is applied to cloud chamber studies of simulated cirrus clouds and, for the first time, to globally distributed measurements from five airborne measurement campaigns conducted between 2011 and 2017 during spring and summer covering regions from the Tropics to the Arctic. The observations of the ice crystal submicron mesoscopic complexity are linked with-to measurements of the ice particle angular light-scattering function performed with two instruments at various geographical locations in the southern and northern hemisphere with two polar nephelometers, the Particle Habit Imaging and Polar Scattering (PHIPS) probe, and the Polar Nephelometer (PN). In two cases the crystal complexity measurements and the angular light-scattering measurements were conducted simultaneously on the same ice particle population. These measurement results populations. The measurement methods and locations are discussed in Sect. 2 and the results in Sect. 3. To assess the significance of the observations to the magnitude of the SWCRE, the measured cloud angular scattering function was parameterized and the new parameterization was tested in the ECHAM-HAM global climate model, and compared against results generated by the standard parameterization. The respective results of the model run-simulations are discussed in Sect. 4.

## 2 Methods

### 2.1 Ice particle complexity analysis

The sub-micron-scale-crystal-mesoscopic complexity of individual sub-50  $\mu\text{m}$  ice particles was determined using the Small-Ice Detector Mark 3 (SID-3) instrument (Kaye et al., 2008). The SID-3 instrument (Kaye et al., 2008), which records the spatial intensity distribution of the coherent laser light scattered in the angular range of 7 to 23° as a two-dimensional (2-D) scattering pattern. Representative examples from the of respective scattering patterns are shown in Fig. 1. The crystal complexity is quantified from the 2-D scattering patterns using a grey-level co-occurrence matrix (GLCM) method (Lu et al., 2006). This method approach was developed for industrial quality control of surface treatment processes but, and was later adapted for analysis of complexity features of three-dimensional ice particles (Ulanowski et al., 2010, 2014; Schnaiter et al., 2016). A more detailed description of the analysis of ice crystal scattering patterns used in this study can be found in Schnaiter et al. (2016).

The GLCM analysis was performed only for scattering patterns that were well illuminated well-illuminated and contained less than 15 % saturated pixels. To be consistent with laboratory studies by Schnaiter et al. (2016), the SID-3 camera gain settings were chosen to be between 175 and 195, and only images within a narrow mean brightness range between 10 and 50 were selected. These steps were taken to minimize image brightness biases on the GLCM analysis results.

Although, the SID-3 has an open geometry to minimize artefacts due to ice particle shattering on the probe housing (McFarquhar et al., 2007; Cotton et al., 2010; Korolev et al., 2011), in-on some occasions shattering events are observed. 2-D scattering patterns from shattered particles can be distinguished from "real" ice particles by analysing the particle time-of-flight (TOF). A typical residence time in the 160  $\mu\text{m}$ -diameter laser beam at an airspeed of 200  $\text{m s}^{-1}$  is 0.8  $\mu\text{s}$  that, divided by the 21 ns clock cycle, corresponds a TOF of 38. In a shattering event, shattered ice crystal fractions pass the sensitive area with short

~~enough of the laser beam with short-enough~~ inter-arrival times, ~~such~~ that the electronics cannot resolve the individual pulses but instead a long TOF value is recorded. To exclude analysing 2-D scattering patterns belonging to shattered particles, the TOF was ~~empirically~~ limited to values below 350. This led to a removal of around 1 % of the 2-D scattering patterns with mean brightness ~~range-ranges~~ between 10 and 50 measured in high altitude clouds. In mixed-phase clouds a higher fraction of  
5 measured 2-D scattering patterns, between 7.5 % and 19 %, were excluded from analysis. ~~The higher fraction of shattering in mixed-phase clouds can be explained by the presence of rimed particles (Jackson et al., 2014).~~

The result of the GLCM analysis is an optical complexity parameter,  $k_e$ , that ~~can have values covers values approximately~~ between 4 and 6 depending on the degree of the actual ~~surface-roughness ice crystals mesoscopic complexity~~. It was shown using both discrete dipole approximation light scattering calculations and cloud chamber simulations, that there is a corre-  
10 lation between the optical complexity parameter  $k_e$  and the physical surface roughness in the range from 0.1 to about 1  $\mu\text{m}$  (~~Schnaiter et al., 2016; Collier et al., 2016~~)(~~Schnaiter et al., 2016~~). Therefore, it is justified to use  $k_e$  as a measure ~~for ice crystal submicron-scale of ice crystal mesoscopic~~ complexity. However, it should be noted that  $k_e$  is an optical parameter and cannot be directly translated into a physical complexity measure or to a distortion parameter used in optical particle models.

~~In addition, the optical complexity parameter cannot differentiate between different types of complexity, that is a roughened ice particle would produce speckles in a similar way as would an ice particle with air inclusions. Therefore, we refrain from using the more established term surface roughness and instead use the term submicron-scale complexity that includes not only surface roughness but also all the other possible causes for the speckles in the 2-D scattering patterns, such as hollowness or air inclusions. In previous studies, such complexity has been referred as the small-scale complexity (Schnaiter et al., 2016; Baran et al., 2017). Here, we suggest to replace the term small with submicron since it is known that the scale of this complexity is in the submicron range.~~  
15  
20

## 2.2 ~~In situ measurements of the angular scattering function~~

### 2.3 ~~Angular light scattering function measurements~~

~~The angular light~~ ~~The angular~~ scattering functions of individual ice particles at 532 nm ~~wavelength~~ were measured with the ~~Particle Habit Imaging and Polar Scattering (PHIPS -) PHIPS~~ aircraft probe (Abdelmonem et al., 2016; Schnaiter et al.,  
25 2018). PHIPS is capable of measuring the angular ~~light~~ scattering function of ~~single-individual~~ particles from 18 to 170° with a repetition rate ~~of 20 kHz as high as 13 kHz~~. The particle size range covered is from 10  $\mu\text{m}$  to approximately 1 mm in diameter. Simultaneously, a stereoscopic image is taken for a sub-sample of particles. Examples of PHIPS images of tropical ice particles ~~is seen are presented~~ in Fig. 1. ~~Before analysis, particles corresponding to shattering events were removed by calculating particle inter-arrival times and removing particle pairs with inter-arrival times less than 1 ms.~~

30 The angular ~~light~~ scattering measurements at 804 nm ~~wavelength~~ were performed with the ~~airborne Polar Nephelometer (PN -) (Gayet et al., 1997; Crépel et al., 1997)~~ PN (~~Gayet et al., 1997; Crépel et al., 1997~~). The PN measures the angular scattering coefficients of particle populations by integrating the measured signals of each detector over a period selected by the operator (typically 100 ms). The particle size range ~~covered~~ is from few micrometres to 1 mm ~~in diameter~~. The scattering angles of

PN cover ~~angles-values~~ from 15° to 162° with ~~an-angular-a~~ resolution of 3.5°. It is not possible to correct the PN data for shattering artefacts, but it has been estimated that shattering artefacts contribute less than 25% to the total extinction signal (Mioche et al., 2017).

### 2.3 Cloud chamber experiments

5 Cloud chamber ~~simulation~~ experiments were performed to study the effect of growth conditions to the ice crystal ~~submicron~~  
~~scale-complexity~~. ~~The cloud chamber simulation mesoscopic complexity.~~ These experiments were performed at the AIDA  
cloud simulation chamber of Karlsruhe Institute of Technology during a series of **Rough ICE** (RICE) experiments. A general  
description of the AIDA facility and instrumentation can be found in several publications (e.g. Möhler et al., 2005; Wagner  
et al., 2011; Schnaiter et al., 2012) and the detailed description of the RICE experiments can be found in Schnaiter et al.  
10 (2016) ~~where the laboratory results from the RICE campaigns are published.~~ Here, we compare field results of ~~submicron scale~~  
~~ice crystal~~ complexity measurements to four laboratory ~~simulation~~ experiments from Schnaiter et al. (2016) that represent  
simulations of pristine, pristine to medium complex, medium complex to severe complex, and severe complex ice crystals  
(Table 1). ~~The experimental procedure is briefly summarized below:-~~

Each simulation experiment started with a pre-cooled and pre-humidified chamber (temperature of -50°C) ~~and pre-humidified~~  
15 ~~( $RH_{ice}$  and relative humidity with respect to ice,  $RH_{ice}$ , of 100%) chamber.~~ Before the experiment, the chamber was filled with  
either sulphuric acid solution droplets for simulations of homogeneous freezing, or with soot aerosol particles for simulations  
of heterogeneous deposition mode freezing. In the first experiment phase the aerosol was activated by expanding the cham-  
ber volume through ~~chamber~~-evacuation. During the initial activation, the ice particle growth conditions cannot be controlled  
and, therefore, a subsequent sublimation is needed to remove any morphological features related to the initial growth. In the  
20 second phase, the ice particles were reduced in size before they ~~are-were~~, in the third experiment phase, re-grown at a sta-  
ble ice supersaturation. During the re-growth period the ice particles were analyzed in terms of their ~~submicron-mesoscopic~~  
complexity.

### 2.4 Sampled clouds and definitions

Field measurements of ice crystal ~~sub-micron-mesoscopic~~ scale complexity were performed between 2011 and 2017 in the  
25 ~~the~~-Mid-latitude Airborne Cirrus Properties Experiment (MACPEX) (Jensen et al., 2013), ~~in~~-the Mid-Latitude Cirrus (ML-  
CIRRUS) campaign (Voigt et al., 2017), ~~in~~-the Aerosol, Cloud, Precipitation, and Radiation Interactions and Dynamics of  
Convective Cloud Systems Cloud processes of the main precipitation systems in Brazil: A contribution to cloud resolving  
modeling and to the GPM (Global Precipitation Measurement) (ACRIDICON-CHUVA) campaign (Wendisch et al., 2016),  
~~in~~-the Radiation-Aerosol-Cloud Experiment in the Arctic Circle (RACEPAC) campaign (Costa et al., 2017) ~~and in the Arctic~~  
30 ~~Clouds – Characterization of Ice, aerosol Particles and Energy fluxes, and the Arctic Cloud Observations Using airborne~~  
~~measurements during polar Day~~ (ACLOUD) campaign (Wendisch and et al., 2018). The field measurements of angular light  
scattering functions were performed between 1998 and 2017 in the Interhemispheric differences in Cirrus properties from  
Anthropogenic emissions (INCA) project (Shcherbakov et al., 2005), ~~in~~-the mid-latitude campaign CIRRUS'98 (Jourdan et al.,

2003), ~~in~~ the Arctic Study on Tropospheric Aerosol and Radiation (ASTAR) campaign (Jourdan et al., 2010), ~~in~~ the Contrail and Cirrus Experiments (CONCERT) 1 and 2 (Chauvigné et al., 2018), ~~in~~ the tropical campaign ACRIDICON-CHUVA, ~~in~~ the Airborne Research Instrumentation Testing Opportunity (ARISTO2017), ~~in the arctic~~ the Arctic campaign ACLOUD and ~~in~~ the Southern Ocean Clouds, Radiation, Aerosol Transport Experimental Study (SOCRATES).

5 In this paper the microphysical and optical properties of ice particles in high altitude clouds, in boundary layer stratocumulus clouds, and in one nimbostratus cloud are reported. The temperature ranges covered in each campaign are shown in Table 2. High altitude clouds were sampled in the tropical campaign ACRIDICON-CHUVA, in the mid-latitude campaigns ML-CIRRUS, MACPEX, ARISTO 2017, CIRRUS'98 and CONCERT, as well as in the Southern Ocean campaign SOCRATES, and in the northern and southern hemispheric campaign INCA. From these ~~campaigns~~ observations, only segments in fully  
10 glaciated parts were selected for the analysis. ~~Sometimes these~~ This included measurements above  $-40^{\circ}\text{C}$  and, therefore, in this study a more general term ice clouds instead of cirrus clouds is used.

Boundary layer stratocumulus clouds were sampled in the ~~arctic~~ Arctic campaigns RACEPAC and ACLOUD, and in the Southern Ocean campaign SOCRATES. Different approaches were applied to select ~~only ice particles to~~ ice particles for the analysis. For the SID-3, a manual inspection of the single particle ~~2D-2-D~~ scattering patterns was performed for the RACEPAC  
15 and ACLOUD flights, where ice was observed. The complexity analysis was performed only for scattering patterns classified manually as ice. To calculate a representative angular scattering function for boundary layer stratocumulus ice particles, the PHIPS single particle angular scattering functions from the ACLOUD and SOCRATES campaigns were first analyzed for their shape. The shape of the rainbow feature, that is the slope between  $106^{\circ}$  and  $138^{\circ}$ , was used to discriminate between liquid droplets and ice particles. Only particles that were classified as ice using this algorithm were included in the analysis.  
20 In ~~these~~ the Arctic campaigns, all the analyzed ice particles were measured in a mixed-phase environment. Therefore, the term Arctic mixed-phase ice is used to label the PHIPS measurements. The PHIPS measurements in the Southern Ocean campaign SOCRATES includes ice particles sampled both in high altitude clouds and in boundary layer stratocumulus (mixed-phase) clouds. In this paper, one representative angular scattering function for Southern Ocean SOCRATES campaign is shown.

An ~~arctic~~ Arctic mixed-phase nimbostratus cloud was sampled during the ASTAR campaign. To retrieve a representative  
25 ice particle angular scattering function for ~~arctic~~ Arctic ice particles, principal component analysis (Jourdan et al., 2003) was performed on the PN data measured at the glaciated top of this system. Since the cloud top was almost fully glaciated (Jourdan et al., 2010), the measurements are labeled in this paper as ~~arctic~~ Arctic ice cloud.

## 2.5 Description of the ECHAM-HAM model.

In our study, we used the ECHAM6.3-HAM2.3 global aerosol-climate model (based on Neubauer et al. (2014) with modifica-  
30 tions). A 10-year simulation with  $1.9^{\circ} \times 1.9^{\circ}$  horizontal resolution with 47 vertical levels was conducted from 2003 to 2012 after 3 months of spin-up time. The meteorology is nudged to ERA-Interim data (Dee et al., 2011) and sea surface temperature and sea ice cover were taken from observations. ~~The SWCRE of the ice clouds was diagnosed by double radiation calls, once with the standard model parameterization for the short-wave asymmetry factors of ice clouds and once with the new parameterization. Radiative~~ In the model the radiative transfer is computed for 14 ~~short-wave~~ short wave bands (and 16 long-

wave bands) (Pincus and Stevens, 2013). A competition between homogeneous and heterogeneous nucleation and pre-existing ice crystals (Kuebbeler et al., 2014; Gasparini and Lohmann, 2016) is considered. Enhancements in the vertical velocity over orography (Joos et al., 2008) are accounted for in the formation of cirrus clouds.

5 The ECHAM-HAM model is used to calculate the SWCRE of the ice clouds, which is computed online by calling the radiation subroutine twice. The first call is with clouds (all-sky) and the second call is without clouds (clear-sky) in the atmosphere. The first call uses the standard model parameterization for the short wave asymmetry factors of ice clouds. The radiative fluxes from this call to the radiation subroutine are used to advance the model simulations. The cloud radiative effects are computed as the difference between the all-sky minus the clear-sky fluxes. To estimate the change in SWCRE by changing the short wave asymmetry factors of ice clouds an additional (third) call to the radiation subroutine is conducted. The additional  
10 (diagnostic) call to the radiation subroutine is identical to the first call except for using the new parameterization for the short wave asymmetry factors of ice clouds. The radiative fluxes from this additional call are only diagnostic. The SWCRE using the new parameterization for the short wave asymmetry factors of ice clouds is computed from the difference in SW radiative flux at the top of the atmosphere from the additional call and the cloud-free SW radiative flux at the top of the atmosphere.

### 3 **In-situ** In situ measurements

#### 15 3.1 Globally distributed **in-situ** in situ observations of ice crystal **submicron** mesoscopic complexity

The tracks of the measurement flights, where ice crystal mesoscopic complexity was studied, are shown in Fig. 2. The southernmost dataset of tropical ice clouds, collected during ACRIDICON-CHUVA campaign, consists mainly of measurements in anvil cirrus, but includes also two cases of synoptic cirrus. The dominant ice crystal habits in the anvil cirrus were found to be plates and aggregates of plates, whereas synoptic cirrus was composed of bullet rosettes and columnar ice crystals (examples of  
20 ice particles in a tropical in-situ in situ cirrus can be found in Fig. 1). The observations of the crystal habits agree with previous observations in convective and synoptic systems (McFarquhar and Heymsfield, 1996; Heymsfield et al., 2002; Connolly et al., 2005; Lawson et al., 2006). In contrast to the tropical cirrus, the ice crystals measured in the ML-CIRRUS campaign were formed in more moderate updrafts in synoptic systems, such as warm conveyor belts or in the jet stream. During MACPEX, the second campaign in mid-latitudes analyzed here, dominant cirrus types were either anvil or jet stream cirrus associated with  
25 spring storm systems (Schmitt et al., 2016b). The northernmost campaigns targeted springtime Arctic boundary layer stratocumulus clouds from northern Canada (RACEPAC) and from Svalbard, Norway (ACLOUD). In ACLOUD, the ice crystals were found at temperatures between  $-3^{\circ}\text{C}$  and  $-10^{\circ}\text{C}$ , where the most common ice crystal shapes were (hollow) rimed needles or plates (Schnaiter et al., 2018).

Only ice crystals in the sub- $50\ \mu\text{m}$  size range were selected from the data obtained during these campaigns. In this size range,  
30 ice particles are single crystals (Schmitt et al., 2016a) and, therefore, complexity is **caused-by-submicron-scale-phenomena-and-not-observed-in-the-mesoscopic-scale-and-is-not-caused** by aggregate structures. Based on laboratory calibrations (Schnaiter et al., 2016) the measured ice crystals can be divided into pristine ( $k_e < 4.6$ ) and complex ( $k_e \geq 4.6$ ) **crystals**. Statistical analysis of the single particle complexity parameters measured in the different campaigns are shown in Fig. 3. This analysis reveals

that a majority, between 61 and 81%, of the ice crystals with sizes below 50  $\mu\text{m}$ , can be classified as complex with median complexity parameters above the defined threshold of  $k_e \geq 4.6$ . In spite of the obvious differences in the ice crystal habits due to the different formation pathways, the median complexity parameters have similar values in all campaigns. The maximum difference in the median complexity parameter was found 0.23 that roughly corresponds to a change of 0.05 in distortion parameter ( $\sigma$ ) (Schnaiter et al., 2016) or 0.04  $\mu\text{m}$  in physical surface roughness (Lu et al., 2006).

Even though the method is limited to the study of ~~sub-micron-mesosopic~~ scale complexity of small ( $< 50 \mu\text{m}$ ) ice particles, it can be postulated that the results give indications also for the structural complexity of ice particles larger than 50  $\mu\text{m}$ . Larger ice particles are frequently aggregates, composed of small single habits whose ~~submicron-mesosopic~~ scale complexity can be measured (Schmitt et al., 2016b). It can be assumed that an aggregated ice crystal has the same or even higher degree of ~~submicron-mesosopic~~ scale complexity as the single habits composing it and, therefore, the asymmetry factor of aggregated crystals is similar or lower than that of the component particles (Yang et al., 2013; Um and McFarquhar, 2009). For example, light scattering calculations have shown that the scattering properties of aggregated hexagonal ice crystals differ only little (around 0.3% at 550 nm) from those of their component particles (Um and McFarquhar, 2009).

### 3.2 Comparison of the field observations to laboratory simulation experiments

In Fig. 3, the atmospheric measurements are compared to four laboratory cirrus cloud experiments performed in the AIDA cloud chamber. In the cloud chamber experiments ice crystals were nucleated either homogeneously or heterogeneously at temperatures around  $-50^\circ\text{C}$ , with a subsequent growth at a defined ice saturation ratio ( $S_{ice}$ ) ranging from near ice saturation to 30% ice supersaturation (Schnaiter et al., 2016). The homogeneous freezing case (AIDA hom.) resulted in the highest degree of ~~submicron-mesosopic~~ scale complexity (median  $k_e$  of 5.33) even at moderate growth conditions ( $S_{ice}$  of 1.1) whereas the degree of ~~submicron-mesosopic~~ scale complexity in the case of heterogeneous freezing (AIDA het.) was dependent on the ice supersaturation ratio during crystal growth. The measured median  $k_e$  values were 4.91, 4.68 and 4.22 for experiments where the crystal growth took place at 30%, 20% and 1% supersaturated conditions, respectively. The difference in the physical surface roughness, as defined by Lu et al. (2006), between the AIDA het. 30% and AIDA het. 1% experiments would roughly be 0.12  $\mu\text{m}$ . A similar ~~enhanced-submicron-scale-complexity-of~~ enhancement in mesoscopic scale complexity in homogeneously formed ice crystals has previously been found in mid-latitude cirrus (Ulanowski et al., 2014), and can be partly explained by an increased stacking disorder of homogeneously nucleated ice crystals (Malkin et al., 2012). The median and the interquartile range of the  $k_e$  from the field observations agree best with the laboratory simulations of heterogeneous freezing where ice crystals were grown at relatively high  $S_{ice}$  of 1.3 (Fig. 3). However, it has to be taken into account that in the atmosphere ice crystals can undergo several growth and sublimation cycles that contribute to the formation of additional crystal complexity after the initial growth (~~Magee et al., 2014~~) (Magee et al., 2014; Chou et al., 2018).

### 3.3 Measurements of the angular **light** scattering function

Our field results show that the degree of ice crystal ~~submicron-scale-mesosopic~~ complexity is always above the threshold value of 4.6, and shows less variation with geographical locations than the variations observed in the laboratory simulations. However,



for estimating the ice cloud radiative effect it is crucial to understand how this microphysical observation affects the radiative properties of cirrus and mixed-phase clouds. Fig. 4 shows field and laboratory measurements of volumetric angular ~~light~~-scattering functions at two solar wavelengths for a particle size range from 10  $\mu\text{m}$  to 1 mm in diameter. Each function represents the median over a whole campaign or over one geographical location. The measured angular scattering functions are flat and featureless. Studies with optical particle models (~~Baum et al., 2010; Jourdan et al., 2010; Yang et al., 2013; Liu et al., 2014b, a; Tang et al., 20~~ that the flattening of the angular scattering function at the sideward angles can be reproduced by ice particles with a high degree of ~~submicron-scale~~ crystal complexity, which is in accordance with our observations. More importantly, the ensemble angular ~~light~~-scattering functions at both solar wavelengths are almost identical irrespective of the geographical location. Although ice crystal habits differ significantly in convective outflows, ~~in-situ in situ~~ cirrus or in boundary layer stratocumulus clouds, this shows that their angular ~~light~~-scattering behaviour is governed by the ~~submicron-scale-complexity-mesosopic~~ features of the crystals.

### 3.4 ~~Retrieving asymmetry factor from~~ Comparison of the measured partial phase function: angular scattering functions to a light scattering database

~~An important consequence of severely roughened ice crystals is that the cloud asymmetry factor in the solar spectral range is less than that of pristine ice crystals (Yang et al., 2013). To estimate the asymmetry factor from our measurements, the measured light scattering functions need to be extrapolated. Our approach was to find a best fit to the angular light scattering measurements using a theoretical phase function whose asymmetry factor is known~~ The measured angular scattering functions at the two wavelengths were compared to theoretical phase functions for different habits calculated using the database of Yang et al. (2013). In accordance with our observations, only severely roughened habits were considered in the theoretical calculations. For generation of the theoretical phase functions a representative ~~size distribution for ice particles ice particle size distribution~~ from the ACRIDICON-CHUVA campaign was used. The size distribution was determined from the PHIPS images by analyzing the maximum ~~diameter-dimension~~ of each imaged ice particle using an algorithm developed by Schön et al. (2011). Furthermore, the sensitivity of the ~~theoretical~~ phase function to the assumed size distribution was investigated and it was found that the shape ~~of the~~ phase function was insensitive to small changes in the median diameter. ~~Fig. 5 shows Figs. 5 and 6 show~~ the measured and normalized ~~volumetric~~ angular scattering functions ~~and the theoretical angular scattering functions calculated based on the scattering data base of Yang et al. (2013) and assuming severely roughened particles for 532 and 804 nm and the theoretical phase functions for nine different habits.~~

Based on the comparison, the severely roughened column aggregate model was found to best represent the measurement at ~~both wavelengths. At 532 nm the theoretical calculations agree with the measurements over the whole measurement range, whereas at 804 nm the model predicts slightly higher intensity in the sideward angles between 57° and 126° but is within the measured interquartile range (Fig. 6). The calculated root mean square errors (RMSE) between the severely roughened column aggregate model and the mean of the measurements are the lowest (0.0017 and 0.0014 for 532 nm. Similarly, and 804 nm, respectively) compared to the other models (RMSEs between 0.0022 and 0.0111 for 532 nm, and 0.0037 and 0.0208 for 804 nm). At the angles around exact-backscattering the severely roughened column aggregate model predicts a relatively flat~~

behaviour. However, recent modelling studies have indicated that the scattering intensities around exact backscattering angles should be enhanced due to coherent scattering (e.g. Zhou, 2018). Although this effect can be important for lidar applications, it does not significantly affect the redistribution of the energy in the scattering process and, thus, the magnitude of the asymmetry factor. Furthermore, comparisons of satellite retrievals of cloud polarization properties with light scattering simulations have shown that optical particle models using severely roughened crystals yield the best agreement (Baum et al., 2011; Yang et al., 2013; Tang et al., 2017) and the current MODIS retrievals are based on the same optical particle model of severely roughened hexagonal aggregates that is used here (Platnick et al., 2017). At 804 nm the model predicted slightly higher intensity in the sideward angles between 57° and 126° but was within the measured interquartile range (Fig. 3). Using

#### 4 Estimating the effect of the observed mesoscopic scale complexity to SWCRE

An important consequence of severely roughened and complex ice crystals is that the cloud asymmetry factor in the solar spectral range is lowered compared to pristine ice crystals (e.g. Macke et al., 1996; Yang and Liou, 1998; Liou et al., 2000; Baum et al., 2000). For example, the severely roughened hexagonal aggregate model has relatively low asymmetry factors of 0.750 and 0.754 at 532 nm and 804 nm, respectively, were retrieved.

#### 5 Estimating the effect of the observed submicron scale complexity to SWCRE

for 532 nm and 804 nm, respectively. To understand the relevance of our observations for climate projections, the effect of the observed decrease in the cloud asymmetry parameter on the SWCRE was estimated. The measured angular light scattering function was used to derive a new parameterization of by newly parameterizing the SW asymmetry factors and this parameterization was tested using the optical model with the best fit to our measurements in the ECHAM-HAM global climate model. The current optical parameterization in the ECHAM-HAM model is calculated based on spherical particles using Mie-theory with the exception that the asymmetry factors are scaled down to be more representative for aspherical ice particles. The steps to retrieve this parametrization are discussed the new parametrization are discussed in Sect. 4.1. The sensitivity of a global climate model to the ice particle surface roughness has already been tested in the study of Yi et al. (2013), where the difference in the SWCRE was calculated for assuming first completely smooth and later severely roughened ice particles. Here, we compare the existing standard parameterization of SW asymmetry factors to our new parameterization and, in this way, estimate the uncertainty in the SWCRE due to the failure to adequately consider ice crystal submicron scale complexity.

#### 4.1 Derivation of the new parameterization of the short-wave asymmetry factor for the ECHAM-HAM model and comparison with the standard parameterization.

Parameterizations of the ice crystal shortwave radiative properties are frequently based on possible impact of the observed ice crystal habits and size distributions (e.g. Wyser and Yang, 1998; Yang et al., 2000; McFarquhar et al., 2002; Um and McFarquhar, 2007) with the assumption that a link exists between the ice crystal microphysical and bulk scattering properties. McFarquhar et al. (2002) showed

that different parameterizations using different habits or habit mixtures can cause a significant variance in the asymmetry factor by 0.07 in the wavelength band of 0.25 to 0.69  $\mu\text{m}$ . This variance becomes especially significant for small ice particles, with effective radius below 20  $\mu\text{m}$ , where also the largest uncertainty in the exact particle form exists. Most small ice particles are classified as quasi-spherical particles based on in-situ cloud particle imaging measurements (McFarquhar and Heymsfield, 1996; Stith et al., 2002). However, angular light scattering measurements have shown that the small quasi-spherical particles can have very different asymmetry factors than that of a spherical particle depending on the degree of submicron complexity (Järvinen et al., 2016).

5 mesoscopic scale complexity to the SWCRE.

To overcome the problem of relating the ice crystal bulk scattering properties to measured microphysical properties, in this study a new parameterization of the SW asymmetry factors is developed using direct measurements of the bulk optical properties.

10 properties.

#### 4.1 Derivation of the new parameterization of the short wave asymmetry factor for the ECHAM-HAM model and comparison with the standard parameterization.

Fig. 4 showed that the observed high degree of submicron-mesoscopic scale complexity dominates the angular light scattering function over the ice crystal shape and a uniform angular light scattering function is observed globally at two wavelengths (532 and 804 nm). Therefore, it is justified to use a single-single-habit optical ice particle model assuming severely roughened surfaces to compute the bulk optical properties of ice clouds for the solar wavelength bands not covered by the measurements. The severely roughened hexagonal aggregate optical particle model (Yang et al., 2013) was used to calculate a new parameterization for the SW asymmetry factor for the wavelength bands from 0.23 to 8.02  $\mu\text{m}$ . This model It was found that the severely roughened column aggregate model showed the best fit of the atmospheric measurements performed at a wavelength of 532 nm both wavelengths. At 804 nm the model disagreed slightly with the measurements at the sideward angles (Fig. 5-4). This disagreement indicates that either the severely roughened column aggregate model does not accurately represent the spectral dependence of the asymmetry factors, or could also be related to systematic measurement uncertainties caused by using different measurement systems. However, since we only have information on the ice particle angular scattering properties at two wavelengths at the moment, only one optical particle model is used to parameterize the asymmetry factors.

20 532 nm both wavelengths. At 804 nm the model disagreed slightly with the measurements at the sideward angles (Fig. 5-4). This disagreement indicates that either the severely roughened column aggregate model does not accurately represent the spectral dependence of the asymmetry factors, or could also be related to systematic measurement uncertainties caused by using different measurement systems. However, since we only have information on the ice particle angular scattering properties at two wavelengths at the moment, only one optical particle model is used to parameterize the asymmetry factors.

Gamma particle size distributions with a variance of 0.1 were used to calculate the bulk asymmetry factors at each wavelength for different effective radii ranging from 4 to 124  $\mu\text{m}$ . The comparison of the standard parameterization in ECHAM-HAM for the SW asymmetry factors and the new parameterization using the severely roughened column aggregate model is shown for selective wavelength bands in Fig. 7. Besides the 3.47  $\mu\text{m}$  band, in other wavelength bands As expected, the new asymmetry factors are lower than what is assumed in the standard parameterization. Further, the, except for the 3.47  $\mu\text{m}$  band. Another consequence of the particle roughening is that the size dependence of the asymmetry factor becomes weaker and for submicron wavelength bands sub-micron wavelength bands (0.23, 0.4 and 0.7  $\mu\text{m}$ ) almost no size dependence is observed. It seems that due to mesoscopic complexity the ice cloud asymmetry factors are not so sensitive to habits or particle size, whereas previous studies on smooth ice crystal have shown that different parameterizations using different habits or habit mixtures can cause a significant variance in the asymmetry factor by 0.07 in the wavelength band of 0.25 to 0.69  $\mu\text{m}$  (McFarquhar et al., 2002).

25 Gamma particle size distributions with a variance of 0.1 were used to calculate the bulk asymmetry factors at each wavelength for different effective radii ranging from 4 to 124  $\mu\text{m}$ . The comparison of the standard parameterization in ECHAM-HAM for the SW asymmetry factors and the new parameterization using the severely roughened column aggregate model is shown for selective wavelength bands in Fig. 7. Besides the 3.47  $\mu\text{m}$  band, in other wavelength bands As expected, the new asymmetry factors are lower than what is assumed in the standard parameterization. Further, the, except for the 3.47  $\mu\text{m}$  band. Another consequence of the particle roughening is that the size dependence of the asymmetry factor becomes weaker and for submicron wavelength bands sub-micron wavelength bands (0.23, 0.4 and 0.7  $\mu\text{m}$ ) almost no size dependence is observed. It seems that due to mesoscopic complexity the ice cloud asymmetry factors are not so sensitive to habits or particle size, whereas previous studies on smooth ice crystal have shown that different parameterizations using different habits or habit mixtures can cause a significant variance in the asymmetry factor by 0.07 in the wavelength band of 0.25 to 0.69  $\mu\text{m}$  (McFarquhar et al., 2002).

30 consequence of the particle roughening is that the size dependence of the asymmetry factor becomes weaker and for submicron wavelength bands sub-micron wavelength bands (0.23, 0.4 and 0.7  $\mu\text{m}$ ) almost no size dependence is observed. It seems that due to mesoscopic complexity the ice cloud asymmetry factors are not so sensitive to habits or particle size, whereas previous studies on smooth ice crystal have shown that different parameterizations using different habits or habit mixtures can cause a significant variance in the asymmetry factor by 0.07 in the wavelength band of 0.25 to 0.69  $\mu\text{m}$  (McFarquhar et al., 2002).

This variance becomes especially significant for small ice particles, with effective radius below 20  $\mu\text{m}$ , where also the largest uncertainty in the exact particle shape exists.

#### **4.2 Influence of ice crystal submicron complexity to the cloud shortwave radiative effect**

~~The standard parameterization of the ice particle shortwave asymmetry factors in the ECHAM-HAM global aerosol-climate model (Neubauer et al. (2014) with modifications) was substituted by a new parameterization calculated with the severely roughened column aggregate optical particle model.~~

#### **4.2 Influence of ice crystal mesoscopic complexity to the cloud shortwave radiative effect**

The change in the global SWCRE ~~due to this new parameterization~~ after applying the new parameterization to all ice clouds (cirrus and mixed-phase) is shown in Fig. 8. The global mean change in the SWCRE is  $-1.12 \text{ W m}^{-2}$ , but regionally it can be as large as  $-8 \text{ W m}^{-2}$ . If the new parameterization is applied only for cirrus clouds, the mean change in the SWCRE is slightly lower,  $-1.00 \text{ W m}^{-2}$ . Therefore, the change in the asymmetry factor mostly affects the cirrus SWCRE and, also, the largest effect is found in the tropical regions where also the cirrus occurrence is the highest (e.g. Sassen et al., 2008). Even though the change in the global SWCRE is small compared to the global mean SWCRE of all clouds of about  $-50 \text{ W m}^{-2}$  (Boucher et al., 2013) ~~it is or to the global mean SWCRE of ice clouds of about  $-16.7 \pm 1.7 \text{ W m}^{-2}$  (Hong et al., 2016) it is~~ approximately one fourth of the global mean cirrus SWCRE of  $-4 \text{ W m}^{-2}$  (Gasparini and Lohmann, 2016) and comparable to the total direct radiative effect of aerosols ( $-2.1 \pm 0.7 \text{ W m}^{-2}$ ) (Lacagnina et al., 2017). The ~~decrease in SWCRE~~ enhanced SW cooling might have important implications on understanding the cirrus CRE not only on global but also on regional scale. For example, the increased reflectivity might change our assessment of the sign of the cloud radiative effect by thin cirrus. So far, thin cirrus has been considered to have a modest but positive cloud radiative effect (around  $0.7 \text{ W m}^{-2}$ ) (McFarquhar et al., 2000), but our results suggest that this needs to be reconsidered.

## **5 Conclusions**

Although current satellite retrievals and a growing number of climate models ~~are~~ have already started using optical parameterizations assuming severely roughened ice crystals to reproduce the observed flat angular scattering function of ice particles, this study gives the first direct observational evidence of ice crystal complexity and links it to an angular scattering function with low asymmetry factor. The results presented here show that optical models assuming severe roughness can represent the angular scattering function in many geographical locations ~~and, thus, reduce with sufficient accuracy.~~ Thus, based on observational evidence, the current uncertainty in the degree of surface roughness of natural ice particles (Cole et al., 2014) can significantly be reduced. Moreover, since the ~~degree of submicron-scale complexity ice particle angular scattering functions~~ did not vary significantly between different geographical locations, the ~~use of a single parameterization for asymmetry factor is justified~~ and, thus, this study supports the implementation of parameterizations based on single severely roughened ice habit into the current modelling efforts of ice particle optical properties in future weather forecast and climate models will be simplified.

**In-situ** **In situ** measurements of the **submicron-scale-mesosopic** complexity using the SID-3 **method-instrument** showed that the majority of measured ice crystals can be classified as complex. The limitation of this method is that only small ( $<50\ \mu\text{m}$ ) ice crystals can be analyzed, and no direct evidence of the **submicron-mesosopic** complexity of larger ( $>50\ \mu\text{m}$ ) ice crystals can be obtained. However, the **light-angular** scattering measurements show indirect evidence that larger ice particles are also likely  
5 complex. This can be seen from Fig. 4 by comparing the angular **light**-scattering functions of laboratory generated sub- $50\ \mu\text{m}$  ice particles and that of natural ice particles. Although the field **measurements-observations** include a wider size range of ice crystals from few tens of microns up to a millimetre, no difference can be observed in the shape-sensitive sideward angular scattering behaviour between laboratory generated single habits and field observations.

Our modelling results showed that the observed ice particle **submicron-mesosopic** scale complexity can significantly affect  
10 the SWCRE due to lowering of the cloud asymmetry factor. The magnitude of the change in the SWCRE of  $-1.12\ \text{W m}^{-2}$  is significant, but in order to estimate the role of ice crystal **submicron-mesosopic** scale complexity for climate projections, future simulations with severely roughened ice crystals in a warmer climate are needed.

*Data availability.* The SID-3 complexity analysis results from ML-CIRRUS and ACRIDICON-CHUVA are available from the HALO database (<https://halo-db.pa.op.dlr.de>). The PHIPS data and SID-3 data from other campaigns are available upon request from Martin  
15 Schnaiter ([martin.schnaiter@kit.edu](mailto:martin.schnaiter@kit.edu)).

*Author contributions.* E.J. and M.S. collected and analysed the SID-3 and PHIPS data from aircraft and AIDA campaigns. O.J. provided the PN data. B.Y. and C.L. performed the optical modelling for retrieval of the asymmetry factors and created the new parameterization of the asymmetry factors for the ECHAM-HAM model. D.N. and U.L. performed the ECHAM-HAM model runs. E.J., M.S., O.J., D.N., C.L., M.A., U.L., M.W., G.M. and T.L. were involved in the scientific interpretation and discussion. E.J. wrote the manuscript with help from O.J.  
20 and D.N. All commented on the paper.

*Competing interests.* The authors declare that they have no competing financial interests.

*Acknowledgements.* We gratefully acknowledge Steffen Münch for implementing the used cirrus scheme into ECHAM-HAM. We would also like to thank all participants of the field studies for their efforts, in particular the technical crews of the HALO, AWI Polar 6 and Polar 2, TBM700, DLR Falcon, NASA WB-57 and NSF G-V. This work has received funding from the Helmholtz Research Program Atmosphere  
25 and Climate, the German Research Foundation (DFG grants SCHN 1140/1-1, SCHN 1140/1-2, SCHN 1140/3-1) within the DFG priority program 1294 (HALO), the German Max Planck Society, the CNES (Centre National des Etudes Spatiales) and The Centre National de la Recherche Scientifique – Institut National des Sciences de l’Univers (CNRS-INSU) within the Expecting EarthCare Learning from A-Train (EECLAT) project (contract n°4500054452 BCT\_69 2017), the Swiss National Supercomputing Centre (CSCS, project ID s652), the Swiss

National Science Foundation (project number 200021\_160177) and the National Natural Science Foundation of China (grant no. 41571348) and by the United States National Science Foundation grants 1660544, 1628674 and 1762096. We gratefully acknowledge the National Science Foundation (NSF) for providing access to the HIAPER aircraft during the ARISTO 2017 project and the support from DFG within the Transregional Collaborative Research Center (TR 172) "Arctic Amplification: Climate Relevant Atmospheric and Surface Processes, and Feedback Mechanisms (AC)<sup>3</sup>" for providing access to the AWI Polar-6 aircraft during the ACLOUD project. The ECHAM-HAMMOZ model is developed by a consortium composed of ETH Zürich, Max Planck Institut für Meteorologie, Forschungszentrum Jülich, University of Oxford, the Finnish Meteorological Institute, and the Leibniz Institute for Tropospheric Research, and managed by the Center for Climate Systems Modeling (C2SM) at ETH Zürich.

## References

- Abdelmonem, A., Järvinen, E., Duft, D., Hirst, E., Vogt, S., Leisner, T., and Schnaiter, M.: PHIPS–HALO: the airborne Particle Habit Imaging and Polar Scattering probe–Part 1: Design and operation, *Atmospheric Measurement Techniques*, 9, 3131–3144, 2016.
- Baran, A. and Francis, P.: On the radiative properties of cirrus cloud at solar and thermal wavelengths: A test of model consistency using high-resolution airborne radiance measurements, *Quarterly Journal of the Royal Meteorological Society: A journal of the atmospheric sciences, applied meteorology and physical oceanography*, 130, 763–778, 2004.
- Baran, A., Francis, P., Labonnote, L.-C., and Doutriaux-Boucher, M.: A scattering phase function for ice cloud: Tests of applicability using aircraft and satellite multi-angle multi-wavelength radiance measurements of cirrus, *Q. J. Roy. Meteor. Soc.*, 127, 2395–2416, 2001.
- Baran, A. J.: From the single-scattering properties of ice crystals to climate prediction: A way forward, *Atmospheric Research*, 112, 45–69, 2012.
- Baran, A. J. and Labonnote, L. C.: On the reflection and polarisation properties of ice cloud, *Journal of Quantitative Spectroscopy and Radiative Transfer*, 100, 41–54, 2006.
- Baran, A. J., Hesse, E., and Sourdeval, O.: The applicability of physical optics in the millimetre and sub-millimetre spectral region. Part I: The ray tracing with diffraction on facets method, *Journal of Quantitative Spectroscopy and Radiative Transfer*, 190, 13–25, 2017.
- Baum, B. A., Yang, P., Hu, Y.-X., and Feng, Q.: The impact of ice particle roughness on the scattering phase matrix, *J. Quant. Spectrosc. Radiat. Transfer*, 111, 2534–2549, 2010.
- Baum, B. A., Yang, P., Heymsfield, A. J., Schmitt, C. G., Xie, Y., Bansemmer, A., Hu, Y.-X., and Zhang, Z.: Improvements in shortwave bulk scattering and absorption models for the remote sensing of ice clouds, *Journal of Applied Meteorology and Climatology*, 50, 1037–1056, 2011.
- Boucher, O., Randall, A. D., Bretherton, P., Feingold, C., Forster, G., Kerminen, P., Kondo, V., Liao, Y., Lohmann, H., Rasch, U., et al.: Clouds and aerosols in climate change 2013, in: *The Physical Science Basis. Contribution of Working Group I to the Fifth Assessment Report of the Intergovernmental Panel on Climate Change*, Cambridge University Press Cambridge, United Kingdom and New York, NY, USA, 2013.
- C-Labonnote, L., Brogniez, G., Buriez, J.-C., Doutriaux-Boucher, M., Gayet, J.-F., and Macke, A.: Polarized light scattering by inhomogeneous hexagonal monocrystals: Validation with ADEOS-POLDER measurements, *J. Geophys. Res. Atmos.*, 106, 12 139–12 153, 2001.
- Chauvigné, A., Jourdan, O., Schwarzenboeck, A., Gourbeyre, C., Gayet, J. F., Voigt, C., Schlager, H., Kaufmann, S., Borrmann, S., Mollerker, S., Minikin, A., Jurkat, T., and Schumann, U.: Statistical analysis of contrail to cirrus evolution during the Contrail and Cirrus Experiment (CONCERT), *Atmos. Chem. Phys.*, 18, 9803–9822, 2018.
- Chou, C., Voigtländer, J., Ulanowski, Z., Herenz, P., Bieligk, H., Clauss, T., Niedermeier, D., Hartmann, S., Ritter, G., and Stratmann, F.: Surface roughness during depositional growth and sublimation of ice crystals, *Atmos. Chem. Phys. Discuss.*, 2018, 1–26, <https://www.atmos-chem-phys-discuss.net/acp-2018-254/>, 2018.
- Cole, B., Yang, P., Baum, B., Riedi, J., and L, C.: Ice particle habit and surface roughness derived from PARASOL polarization measurements, *Atmospheric Chemistry and Physics*, 14, 3739–3750, 2014.
- Collier, C., Hesse, E., Taylor, L., Ulanowski, Z., Penttilä, A., and Nousiainen, T.: Effects of surface roughness with two scales on light scattering by hexagonal ice crystals large compared to the wavelength: DDA results, *Journal of Quantitative Spectroscopy and Radiative Transfer*, 182, 225 – 239, <https://doi.org/https://doi.org/10.1016/j.jqsrt.2016.06.007>, <http://www.sciencedirect.com/science/article/pii/S0022407316300802>, 2016.

- Connolly, P., Saunders, C., Gallagher, M., Bower, K., Flynn, M., Choulaton, T., Whiteway, J., and Lawson, R.: Aircraft observations of the influence of electric fields on the aggregation of ice crystals, *Q. J. Roy. Meteor. Soc.*, 131, 1695–1712, 2005.
- Costa, A., Meyer, J., Afchine, A., Luebke, A., Günther, G., Dorsey, J. R., Gallagher, M. W., Ehrlich, A., Wendisch, M., Baumgardner, D., et al.: Classification of Arctic, midlatitude and tropical clouds in the mixed-phase temperature regime, *Atmospheric Chemistry and Physics*, 17, 12219, 2017.
- 5 Cotton, R., Osborne, S., Ulanowski, Z., Hirst, E., Kaye, P. H., and Greenaway, R.: The ability of the Small Ice Detector (SID-2) to characterize cloud particle and aerosol morphologies obtained during flights of the FAAM BAe-146 research aircraft, *Journal of Atmospheric and Oceanic Technology*, 27, 290–303, 2010.
- Crépel, O., Gayet, J.-F., Fournol, J.-F., and Oshchepkov, S.: A new airborne Polar Nephelometer for the measurement of optical and micro-physical cloud properties. Part II: Preliminary tests, in: *Annales Geophysicae*, vol. 15, pp. 460–470, Springer, 1997.
- 10 Dee, D. P., Uppala, S., Simmons, A., Berrisford, P., Poli, P., Kobayashi, S., Andrae, U., Balmaseda, M., Balsamo, G., Bauer, P., et al.: The ERA-Interim reanalysis: Configuration and performance of the data assimilation system, *Quarterly Journal of the royal meteorological society*, 137, 553–597, 2011.
- Diedenhoven, B. v., Cairns, B., Geogdzhayev, I., Fridlind, A., Ackerman, A., Yang, P., and Baum, B.: Remote sensing of ice crystal asymmetry parameter using multi-directional polarization measurements–Part 1: Methodology and evaluation with simulated measurements, *Atmos. Meas. Tech.*, 5, 2361–2374, 2012.
- 15 Doutriaux-Boucher, M., Buriez, J.-C., Brogniez, G., Laurent, C., Baran, A. J., et al.: Sensitivity of retrieved POLDER directional cloud optical thickness to various ice particle models, *Geophys. Res. Lett.*, 27, 109–112, 2000.
- Febvre, G., Gayet, J.-F., Minikin, A., Schlager, H., Shcherbakov, V., Jourdan, O., Busen, R., Fiebig, M., Kärcher, B., and Schumann, U.: On optical and microphysical characteristics of contrails and cirrus, *Journal of Geophysical Research: Atmospheres*, 114, 2009.
- 20 Gasparini, B. and Lohmann, U.: Why cirrus cloud seeding cannot substantially cool the planet, *Journal of Geophysical Research: Atmospheres*, 121, 4877–4893, 2016.
- Gayet, J.-F., Crépel, O., Fournol, J., and Oshchepkov, S.: A new airborne polar Nephelometer for the measurements of optical and micro-physical cloud properties. Part I: Theoretical design, *Annales Geophysicae*, 15, 451–459, 1997.
- 25 Gayet, J.-F., Shcherbakov, V., Mannstein, H., Minikin, A., Schumann, U., Ström, J., Petzold, A., Ovarlez, J., and Immler, F.: Microphysical and optical properties of midlatitude cirrus clouds observed in the southern hemisphere during INCA, *Quarterly Journal of the Royal Meteorological Society*, 132, 2719–2748, 2006.
- Gerber, H., Takano, Y., Garrett, T. J., and Hobbs, P. V.: Nephelometer measurements of the asymmetry parameter, volume extinction coefficient, and backscatter ratio in Arctic clouds, *Journal of the atmospheric sciences*, 57, 3021–3034, 2000.
- 30 Heymsfield, A. J. and Platt, C.: A parameterization of the particle size spectrum of ice clouds in terms of the ambient temperature and the ice water content, *J. Atmos. Sci.*, 41, 846–855, 1984.
- Heymsfield, A. J., Bansemer, A., Field, P. R., Durden, S. L., Stith, J. L., Dye, J. E., Hall, W., and Grainger, C. A.: Observations and parameterizations of particle size distributions in deep tropical cirrus and stratiform precipitating clouds: Results from in situ observations in TRMM field campaigns, *Journal of the atmospheric sciences*, 59, 3457–3491, 2002.
- 35 Hong, Y., Liu, G., and Li, J.-L.: Assessing the radiative effects of global ice clouds based on CloudSat and CALIPSO measurements, *J. Clim.*, 29, 7651–7674, 2016.



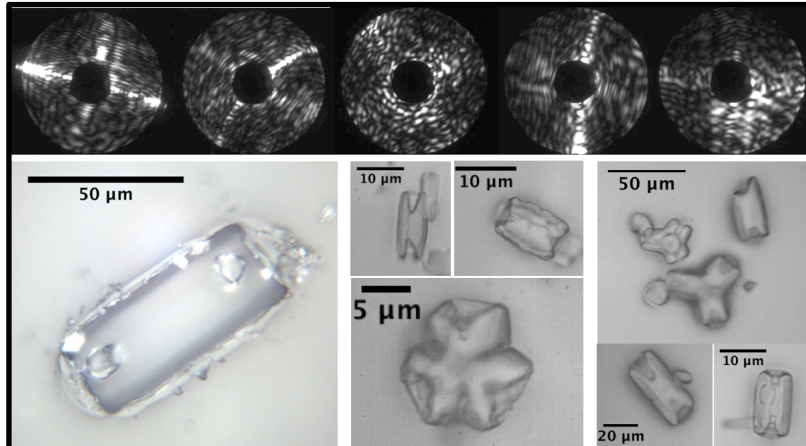
- Jackson, R. C., McFarquhar, G. M., Stith, J., Beals, M., Shaw, R. A., Jensen, J., Fugal, J., and Korolev, A.: An assessment of the impact of antishattering tips and artifact removal techniques on cloud ice size distributions measured by the 2D cloud probe, *Journal of Atmospheric and Oceanic Technology*, 31, 2567–2590, 2014.
- Järvinen, E., Schnaiter, M., Mioche, G., Jourdan, O., Shcherbakov, V. N., Costa, A., Afchine, A., Krämer, M., Heidelberg, F., Jurkat, T., Voigt, C., Schlager, H., NICHMAN, L., Gallagher, M., Hirst, E., Schmitt, C., Bansemer, A., Heymsfield, A., Lawson, P., Tricoli, U., Pfeilsticker, K., Vochezer, P., Möhler, O., and Leisner, T.: Quasi-Spherical Ice in Convective Clouds, *Journal of the Atmospheric Sciences*, 73, 3885–3910, <https://doi.org/10.1175/JAS-D-15-0365.1>, 2016.
- Jensen, E., Lawson, R., Bergman, J., Pfister, L., Bui, T., and Schmitt, C.: Physical processes controlling ice concentrations in synoptically forced, midlatitude cirrus, *Journal of Geophysical Research: Atmospheres*, 118, 5348–5360, 2013.
- 10 Joos, H., Spichtinger, P., Lohmann, U., Gayet, J.-F., and Minikin, A.: Orographic cirrus in the global climate model ECHAM5, *Journal of Geophysical Research: Atmospheres*, 113, 2008.
- Jourdan, O., Oshchepkov, S., Shcherbakov, V., Gayet, J.-F., and Isaka, H.: Assessment of cloud optical parameters in the solar region: Retrievals from airborne measurements of scattering phase functions, *J. Geophys. Res. Atmos.*, 108, 2003.
- Jourdan, O., Mioche, G., Garrett, T. J., Schwarzenböck, A., Vidot, J., Xie, Y., Shcherbakov, V., Yang, P., and Gayet, J.-F.: Coupling of the 15 microphysical and optical properties of an Arctic nimbostratus cloud during the ASTAR 2004 experiment: Implications for light-scattering modeling, *J. Geophys. Res. Atmos.*, 115, 2010.
- Kaye, P. H., Hirst, E., Greenaway, R. S., Ulanowski, Z., Hesse, E., DeMott, P. J., Saunders, C., and Connolly, P.: Classifying atmospheric ice crystals by spatial light scattering, *Opt. Lett.*, 33, 1545–1547, 2008.
- Korolev, A., Isaac, G., and Hallett, J.: Ice particle habits in Arctic clouds, *Geophys. Res. Lett.*, 26, 1299–1302, 1999.
- 20 Korolev, A., Emery, E., Strapp, J., Cober, S., Isaac, G., Wasey, M., and Marcotte, D.: Small ice particles in tropospheric clouds: Fact or artifact? Airborne Icing Instrumentation Evaluation Experiment, *Bulletin of the American Meteorological Society*, 92, 967–973, 2011.
- Kuebbeler, M., Lohmann, U., Hendricks, J., and Kärcher, B.: Dust ice nuclei effects on cirrus clouds, *Atmospheric Chemistry and Physics*, 14, 3027–3046, 2014.
- Lacagnina, C., Hasekamp, O. P., and Torres, O.: Direct radiative effect of aerosols based on PARASOL and OMI satellite observations, 25 *Journal of Geophysical Research: Atmospheres*, 122, 2366–2388, 2017.
- Lawson, R. P., Baker, B., Pilson, B., and Mo, Q.: In situ observations of the microphysical properties of wave, cirrus, and anvil clouds. Part II: Cirrus clouds, *J. Atmos. Sci.*, 63, 3186–3203, 2006.
- Letu, H., Ishimoto, H., Riedi, J., Nakajima, T. Y., C-Labonnote, L., Baran, A. J., Nagao, T. M., and Sekiguchi, M.: Investigation of ice particle habits to be used for ice cloud remote sensing for the GCOM-C satellite mission, *Atmos. Chem. Phys.*, 16, 12 287–12 303, 2016.
- 30 Liou, K., Takano, Y., Yang, P., et al.: Light scattering and radiative transfer in ice crystal clouds: Applications to climate research, *Light Scattering by Nonspherical Particles*, pp. 417–449, 2000.
- Liu, C., Panetta, R. L., and Yang, P.: The effective equivalence of geometric irregularity and surface roughness in determining particle single-scattering properties, *Optics express*, 22, 23 620–23 627, 2014a.
- Liu, C., Yang, P., Minnis, P., Loeb, N., Kato, S., Heymsfield, A., and Schmitt, C.: A two-habit model for the microphysical and optical 35 properties of ice clouds, *Atmos. Chem. Phys.*, 14, 13 719–13 737, 2014b.
- Lu, R.-S., Tian, G.-Y., Gledhill, D., and Ward, S.: Grinding surface roughness measurement based on the co-occurrence matrix of speckle pattern texture, *Appl. Opt.*, 45, 8839–8847, 2006.
- Macke, A., Mueller, J., and Raschke, E.: Single scattering properties of atmospheric ice crystals, *J. Atmos. Sci.*, 53, 2813–2825, 1996.

- Magee, N., Miller, A., Amaral, M., and Cumiskey, A.: Mesoscopic surface roughness of ice crystals pervasive across a wide range of ice crystal conditions, *Atmospheric Chemistry and Physics*, 14, 12 357–12 371, 2014.
- Malkin, T. L., Murray, B. J., Brukhno, A. V., Anwar, J., and Salzmann, C. G.: Structure of ice crystallized from supercooled water, *Proceedings of the National Academy of Sciences*, 109, 1041–1045, 2012.
- 5 McFarquhar, G. M. and Heymsfield, A. J.: Microphysical characteristics of three anvils sampled during the Central Equatorial Pacific Experiment, *J. Atmos. Sci.*, 53, 2401–2423, 1996.
- McFarquhar, G. M., Heymsfield, A. J., Spinhirne, J., and Hart, B.: Thin and subvisual tropopause tropical cirrus: Observations and radiative impacts, *Journal of the Atmospheric Sciences*, 57, 1841–1853, 2000.
- McFarquhar, G. M., Yang, P., Macke, A., and Baran, A. J.: A new parameterization of single scattering solar radiative properties for tropical anvils using observed ice crystal size and shape distributions, *Journal of the atmospheric sciences*, 59, 2458–2478, 2002.
- 10 McFarquhar, G. M., Um, J., Freer, M., Baumgardner, D., Kok, G. L., and Mace, G.: Importance of small ice crystals to cirrus properties: Observations from the Tropical Warm Pool International Cloud Experiment (TWP-ICE), *Geophysical research letters*, 34, 2007.
- Mioche, G., Jourdan, O., Delanoë, J., Gourbeyre, C., Febvre, G., Dupuy, R., Monier, M., Szczap, F., Schwarzenboeck, A., and Gayet, J.-F.: Vertical distribution of microphysical properties of Arctic springtime low-level mixed-phase clouds over the Greenland and Norwegian seas, *Atmos. Chem. Phys.*, 17, 12 845–12 869, 2017.
- 15 Möhler, O., Büttner, S., Linke, C., Schnaiter, M., Saathoff, H., Stetzer, O., Wagner, R., Krämer, M., Mangold, A., Ebert, V., et al.: Effect of sulfuric acid coating on heterogeneous ice nucleation by soot aerosol particles, *J. Geophys. Res. Atmos.*, 110, 2005.
- Neshyba, S., Lowen, B., Benning, M., Lawson, A., and Rowe, P.: Roughness metrics of prismatic facets of ice, *J. Geophys. Res. Atmos.*, 118, 3309–3318, 2013.
- 20 Neubauer, D., Lohmann, U., Hoose, C., and Frontoso, M.: Impact of the representation of marine stratocumulus clouds on the anthropogenic aerosol effect, *Atmos. Chem. Phys.*, 14, 11–997, 2014.
- Pincus, R. and Stevens, B.: Paths to accuracy for radiation parameterizations in atmospheric models, *Journal of Advances in Modeling Earth Systems*, 5, 225–233, 2013.
- Platnick, S., Meyer, K. G., King, M. D., Wind, G., Amarasinghe, N., Marchant, B., Arnold, G. T., Zhang, Z., Hubanks, P. A., Holz, R. E., et al.: The MODIS cloud optical and microphysical products: Collection 6 updates and examples from Terra and Aqua, *IEEE Transactions on Geoscience and Remote Sensing*, 55, 502–525, 2017.
- 25 Sassen, K., Wang, Z., and Liu, D.: Global distribution of cirrus clouds from CloudSat/Cloud-Aerosol lidar and infrared pathfinder satellite observations (CALIPSO) measurements, *J. Geophys. Res. Atmos.*, 113, 2008.
- Schmitt, C. G., Heymsfield, A. J., Connolly, P., Järvinen, E., and Schnaiter, M.: A global view of atmospheric ice particle complexity, *Geophysical Research Letters*, 43, 2016a.
- 30 Schmitt, C. G., Schnaiter, M., Heymsfield, A. J., Yang, P., Hirst, E., and Bansemer, A.: The microphysical properties of small ice particles measured by the Small Ice Detector-3 probe during the MACPEX field campaign, *Journal of the Atmospheric Sciences*, 2016b.
- Schnaiter, M., Büttner, S., Möhler, O., Skrotzki, J., Vragel, M., and Wagner, R.: Influence of particle size and shape on the backscattering linear depolarisation ratio of small ice crystals - cloud chamber measurements in the context of contrail and cirrus microphysics, *Atmos. Chem. Phys.*, 12, 10 465–10 484, 2012.
- 35 Schnaiter, M., Järvinen, E., Vochezer, P., Abdelmonem, A., Wagner, R., Jourdan, O., Shcherbakov, V. N., Schmitt, C. G., Tricoli, U., Ulanowski, Z., and Heymsfield, A. J.: Cloud Chamber Experiments on the Origin of Ice Crystal Surface Roughness in Cirrus Clouds, *Atmos. Chem. Phys.*, 16, 5091–5110, 2016.

- Schnaiter, M., Järvinen, E., Abdelmonem, A., and Leisner, T.: PHIPS-HALO: the airborne particle habit imaging and polar scattering probe – Part 2: Characterization and first results, *Atmospheric Measurement Techniques*, 11, 341–357, <https://doi.org/10.5194/amt-11-341-2018>, <https://www.atmos-meas-tech.net/11/341/2018/>, 2018.
- Schön, R., Schnaiter, M., Ulanowski, Z., Schmitt, C., Benz, S., Möhler, O., Vogt, S., Wagner, R., and Schurath, U.: Particle habit imaging using incoherent light: a first step toward a novel instrument for cloud microphysics, *Journal of Atmospheric and Oceanic Technology*, 28, 493–512, 2011.
- Shcherbakov, V., Gayet, J.-F., Jourdan, O., Minikin, A., Ström, J., and Petzold, A.: Assessment of cirrus cloud optical and microphysical data reliability by applying statistical procedures, *Journal of Atmospheric and Oceanic Technology*, 22, 409–420, 2005.
- Stith, J., Avallone, L., Bansemer, A., Basarab, B., Dorsi, S., Fuchs, B., Lawson, R., Rogers, D., Rutledge, S., and Toohey, D.: Ice particles in the upper anvil regions of midlatitude continental thunderstorms: the case for frozen-drop aggregates, *Atmospheric Chemistry and Physics*, 14, 1973–1985, 2014.
- Sun, W., Loeb, N. G., Videen, G., and Fu, Q.: Examination of surface roughness on light scattering by long ice columns by use of a two-dimensional finite-difference time-domain algorithm, *Appl. Opt.*, 43, 1957–1964, 2004.
- Tang, G., Panetta, R. L., Yang, P., Kattawar, G. W., and Zhai, P.-W.: Effects of ice crystal surface roughness and air bubble inclusions on cirrus cloud radiative properties from remote sensing perspective, *Journal of Quantitative Spectroscopy and Radiative Transfer*, 195, 119–131, 2017.
- Ulanowski, Z., Hesse, E., Kaye, P. H., and Baran, A. J.: Light scattering by complex ice-analogue crystals, *Journal of Quantitative Spectroscopy and Radiative Transfer*, 100, <https://doi.org/10.1016/j.jqsrt.2005.11.052>, 2006.
- Ulanowski, Z., Kaye, P. H., Hirst, E., and Greenaway, R.: Light scattering by ice particles in the Earth’s atmosphere and related laboratory measurements, in: *Procs 12th Int Conf on Electromagnetic and Light Scattering*, University of Helsinki, 2010.
- Ulanowski, Z., Kaye, P. H., Hirst, E., Greenaway, R., Cotton, R. J., Hesse, E., and Collier, C. T.: Incidence of rough and irregular atmospheric ice particles from Small Ice Detector 3 measurements, *Atmos. Chem. Phys.*, 14, 1649–1662, 2014.
- Um, J. and McFarquhar, G. M.: Single-scattering properties of aggregates of bullet rosettes in cirrus, *Journal of applied meteorology and climatology*, 46, 757–775, 2007.
- Um, J. and McFarquhar, G. M.: Single-scattering properties of aggregates of plates, *Quarterly Journal of the Royal Meteorological Society*, 135, 291–304, 2009.
- Voigt, C., Schumann, U., Minikin, A., Abdelmonem, A., Afchine, A., Borrmann, S., Boettcher, M., Buchholz, B., Bugliaro, L., Costa, A., Curtius, J., Dollner, M., Dörnbrack, A., Dreiling, V., Ebert, V., Ehrlich, A., Fix, A., Forster, L., Frank, F., Fütterer, D., Giez, A., Graf, K., Groß, J.-U., Groß, S., Heinold, B., Hüneke, T., Järvinen, E., Jurkat, T., Kaufmann, S., Kenntner, M., Klingebiel, M., Klimach, T., Kohl, R., Krämer, M., Krisna, T. C., Luebke, A., Mayer, B., Mertes, S., Molleker, S., Petzold, A., Pfeilsticker, K., Port, M., Rapp, M., Reutter, P., Rolf, C., Rose, D., Sauer, D., Schäfler, A., Schlage, R., Schnaiter, M., Schneider, J., Spelten, N., Spichtinger, P., Stock, P., Weigel, R., Weinzierl, B., Wendisch, M., Werner, F., Wernli, H., Wirth, M., Zahn, A., Ziereis, H., and Zöger, M.: ML-CIRRUS - The airborne experiment on natural cirrus and contrail cirrus with the high-altitude long-range research aircraft HALO, *Bull. Amer. Meteor. Soc.*, 98, 271–288, 2017.
- Wagner, R., Möhler, O., Saathoff, H., Schnaiter, M., and Leisner, T.: New cloud chamber experiments on the heterogeneous ice nucleation ability of oxalic acid in the immersion mode, *Atmos. Chem. Phys.*, 11, 2083–2110, 2011.
- Wendisch, M. and et al.: The Arctic Cloud Puzzle: Using ALOUD/PASCAL Multi-Platform Observations to Unravel the Role of Clouds and Aerosol Particles in Arctic Amplification, Submitted to *Bull. Am. Meteorol. Soc.*, 2018.

- Wendisch, M., Pöschl, U., Andreae, M. O., Machado, L. A., Albrecht, R., Schlager, H., Rosenfeld, D., Martin, S. T., Abdelmonem, A., Afchine, A., et al.: The ACRIDICON-CHUVA campaign: Studying tropical deep convective clouds and precipitation over Amazonia using the new German research aircraft HALO, *Bull. Amer. Meteor. Soc.*, 97, 1885–1908, 2016.
- Wyser, K. and Yang, P.: Average ice crystal size and bulk short-wave single-scattering properties of cirrus clouds, *Atmospheric research*, 49, 315–335, 1998.
- Yang, P. and Liou, K.: Single-scattering properties of complex ice crystals in terrestrial atmosphere, *Beitrage zur Physik der Atmosphäre—Contributions to Atmospheric Physics*, 71, 223–248, 1998.
- Yang, P., Liou, K., Wyser, K., and Mitchell, D.: Parameterization of the scattering and absorption properties of individual ice crystals, *Journal of Geophysical Research: Atmospheres*, 105, 4699–4718, 2000.
- 10 Yang, P., Kattawar, G. W., Hong, G., Minnis, P., and Hu, Y.: Uncertainties associated with the surface texture of ice particles in satellite-based retrieval of cirrus clouds—Part I: Single-scattering properties of ice crystals with surface roughness, *IEEE Trans. Geosci. Remote Sens.*, 46, 1940–1947, 2008.
- Yang, P., Bi, L., Baum, B. A., Liou, K.-N., Kattawar, G. W., Mishchenko, M. I., and Cole, B.: Spectrally consistent scattering, absorption, and polarization properties of atmospheric ice crystals at wavelengths from 0.2 to 100  $\mu$  m, *Journal of the Atmospheric Sciences*, 70, 330–347, 2013.
- 15 Yi, B., Yang, P., Baum, B. A., L’Ecuyer, T., Oreopoulos, L., Mlawer, E. J., Heymsfield, A. J., and Liou, K.: Influence of Ice Particle Surface Roughening on the Global Cloud Radiative Effect, *Journal of the Atmospheric Sciences*, 70, <https://doi.org/10.1175/JAS-D-13-020.1>, 2013.
- Yi, B., Yang, P., Liu, Q., Delst, P., Boukabara, S.-A., and Weng, F.: Improvements on the ice cloud modeling capabilities of the Community Radiative Transfer Model, *Journal of Geophysical Research: Atmospheres*, 121, 2016.
- 20 Zhou, C.: Coherent backscatter enhancement in single scattering, *Opt. Express*, 26, A508–A519, 2018.

## Laboratory Produced Ice Particles



## Ice Particles in a Tropical Cirrus

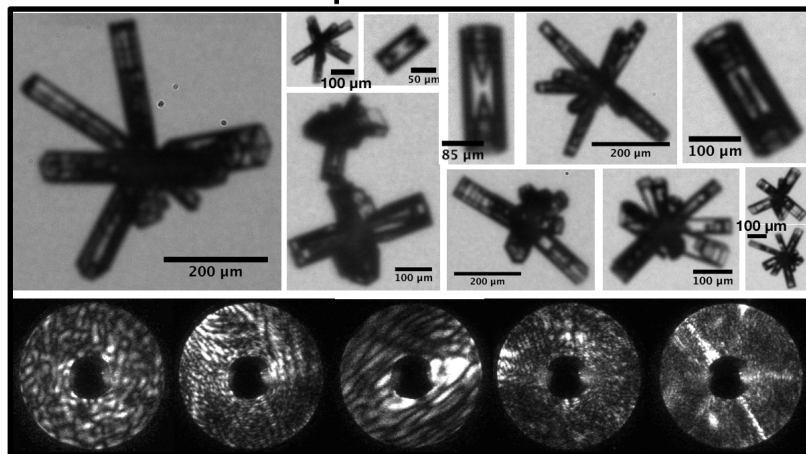


**Figure 1.** Hexagonal ice crystals and 2D diffraction patterns measured in laboratory simulations at  $-50^{\circ}\text{C}$  (upper panel) and in tropical cirrus at  $-60^{\circ}\text{C}$  (lower panel). The microscopic images of the laboratory produced ice crystals are from ice crystal replicas and the tropical cirrus ice particles were imaged in flight using bright field microscopy. The 2D diffraction patterns were measured simultaneously from the same particle population.

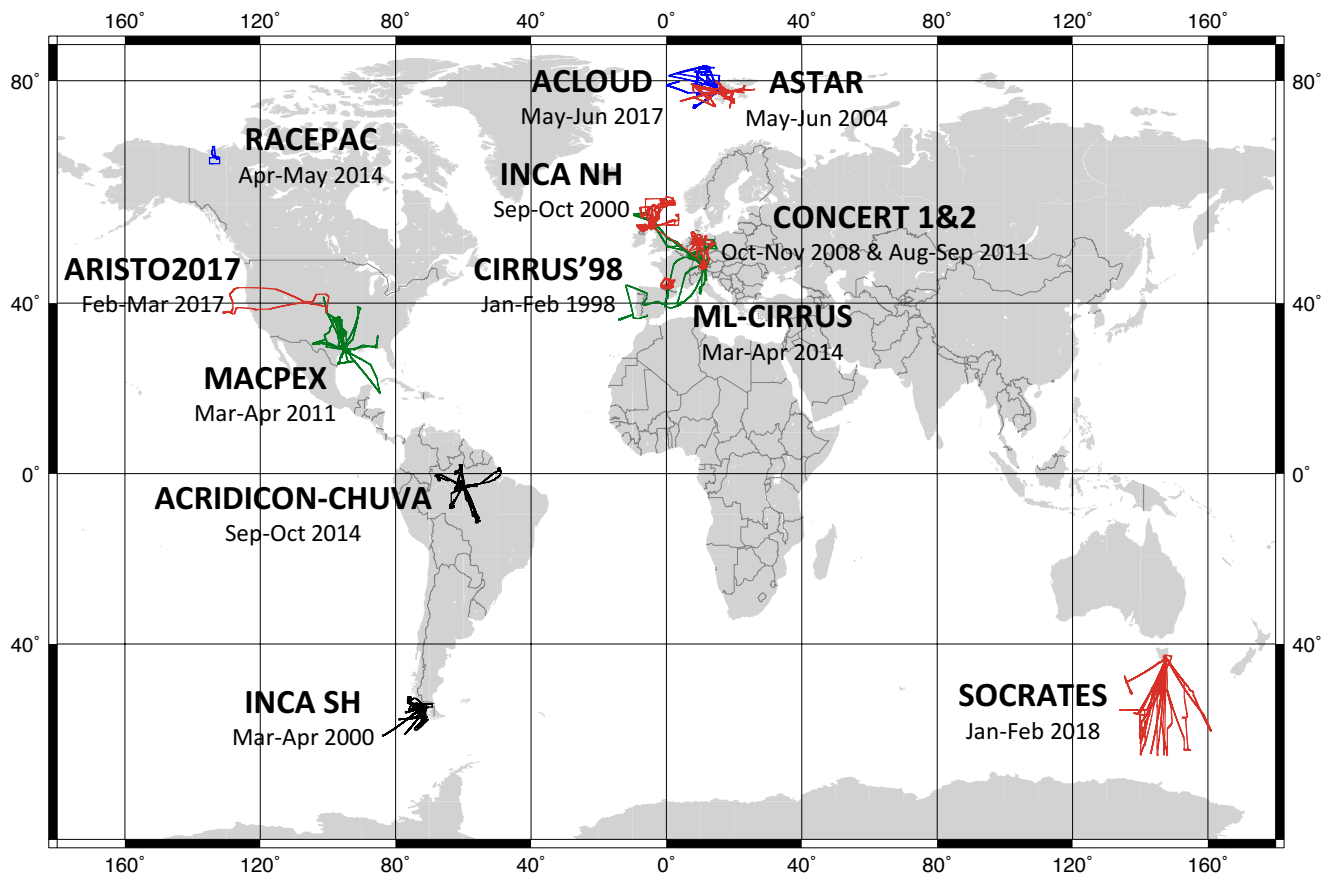


**Figure 2.** Flight trajectories of all campaigns included in this study. Trajectories of the campaigns where ice crystal submicron-mesoscopic scale complexity was investigated are marked with black, purple and blue matching the colours used in Fig. 3. Trajectories of the campaigns where only angular light-scattering function was measured are marked with red. Simultaneous submicron-mesoscopic scale complexity measurements and angular light-scattering measurements were performed in ACRIDICON-CHUVA and ACLOUD campaigns.

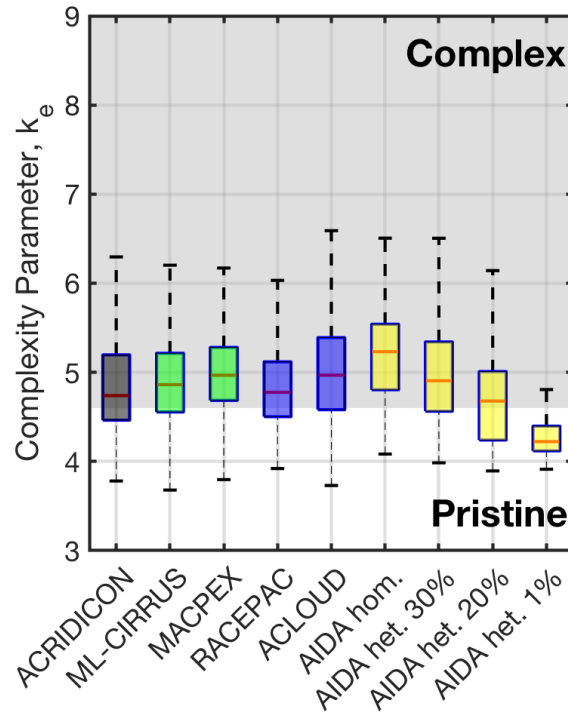


**Figure 3.** Statistical analysis of ice crystal complexity from all measured ice particles in the aircraft campaigns and from four AIDA cloud chamber simulation experiments. The box edges represent the 25 and 75% quartiles and the dashed lines the 5 and 95% quartiles. The red lines represent the median values. The grey area indicates the range of the complexity parameter in which the ice crystals are characterized to be complex. The median complexity parameters were found to be 4.74 in ACRIDICON-CHUVA, 4.86 in ML-CIRRUS, 4.97 in MACPEX, 4.78 in RACEPAC and 4.97 in A CLOUD.

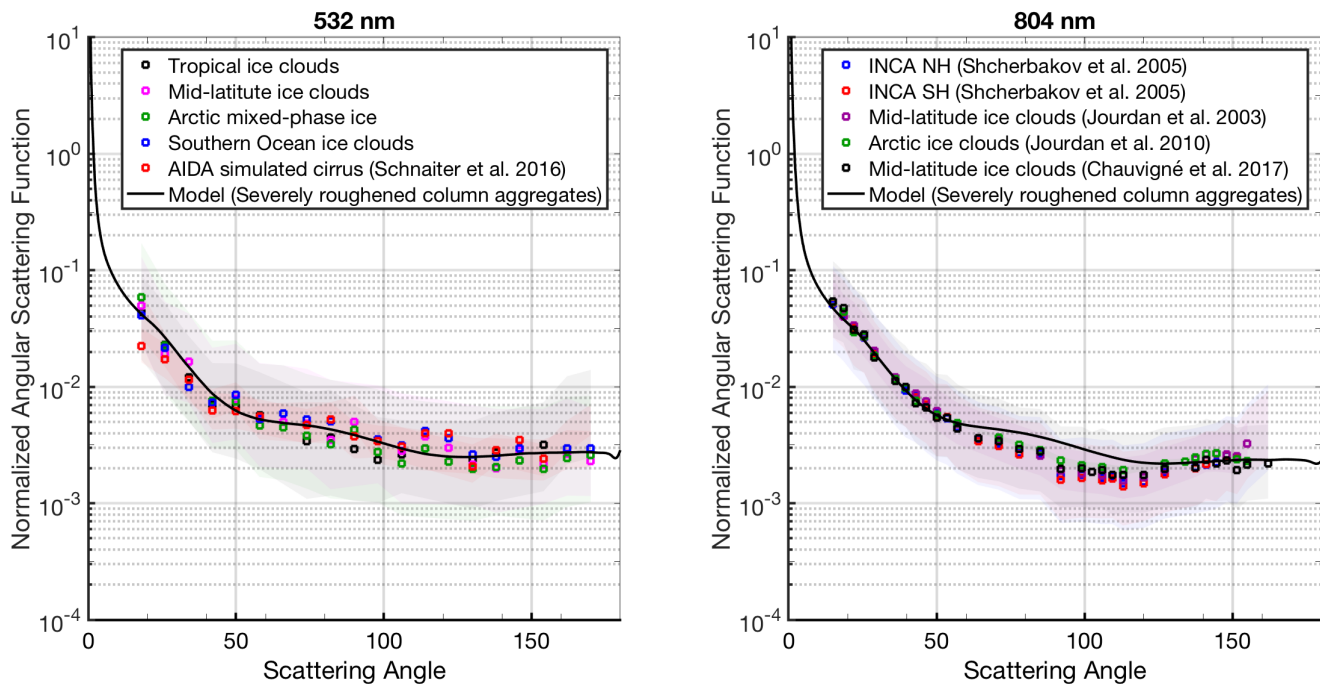


**Figure 4.** Ensemble angular **light**-scattering functions of natural and laboratory generated ice particles measured at two wavelengths. Each function represents the median angular scattering function over a single campaign and is normalized to the total intensity between  $18^\circ$  and  $170^\circ$ . The shaded area represents the interquartile range. The measurements at 532 nm in tropical cirrus, Arctic boundary layer stratocumulus clouds as well as the measurements in laboratory-simulated cirrus were gathered together with the complexity measurements in the ACRIDICON-CHUVA, ACLOUD and AIDA campaigns. The mid-latitude and Southern Ocean measurements at 532 nm were measured during the ARISTO campaign in 2017 and during the SOCRATES campaign, respectively. The measurements at 804 nm were measured between 1997–2011 in the CIRRUS'98, INCA, ASTAR and CONCERT aircraft campaigns.



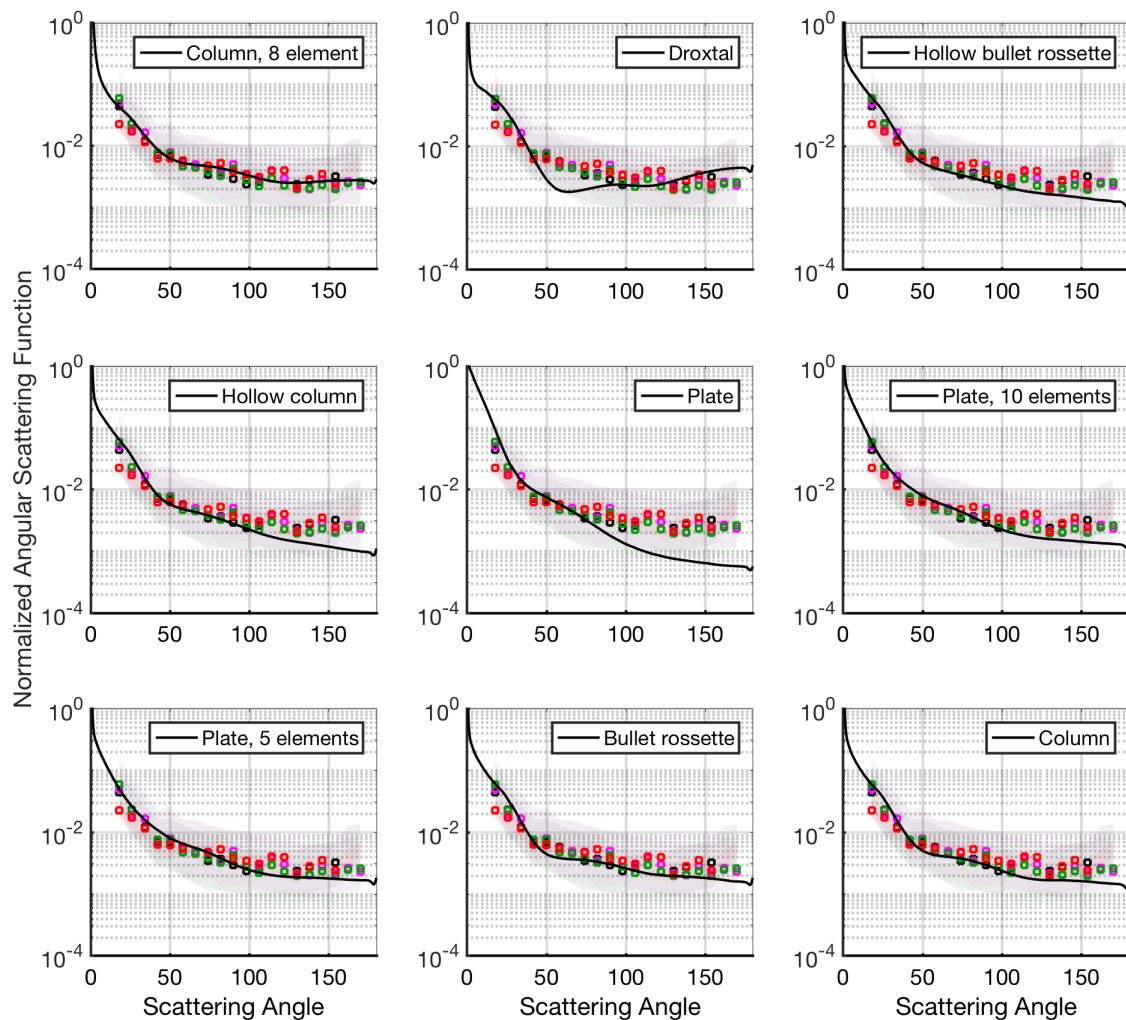


**Figure 5.** A comparison of the measured angular light-scattering functions at 532 nm ([data from first panel of Fig. 4](#)) and [theoretical phase functions](#) for different [optical particle models from habits](#) calculated using the database of Yang et al. (2013) and assuming a size distribution as measured during the ACRIDICON-CHUVA campaign. All [models use calculations were performed assuming](#) severely roughened surfaces. Both the measurements and the model results are normalized to the total intensity between  $18^\circ$  and  $170^\circ$ .

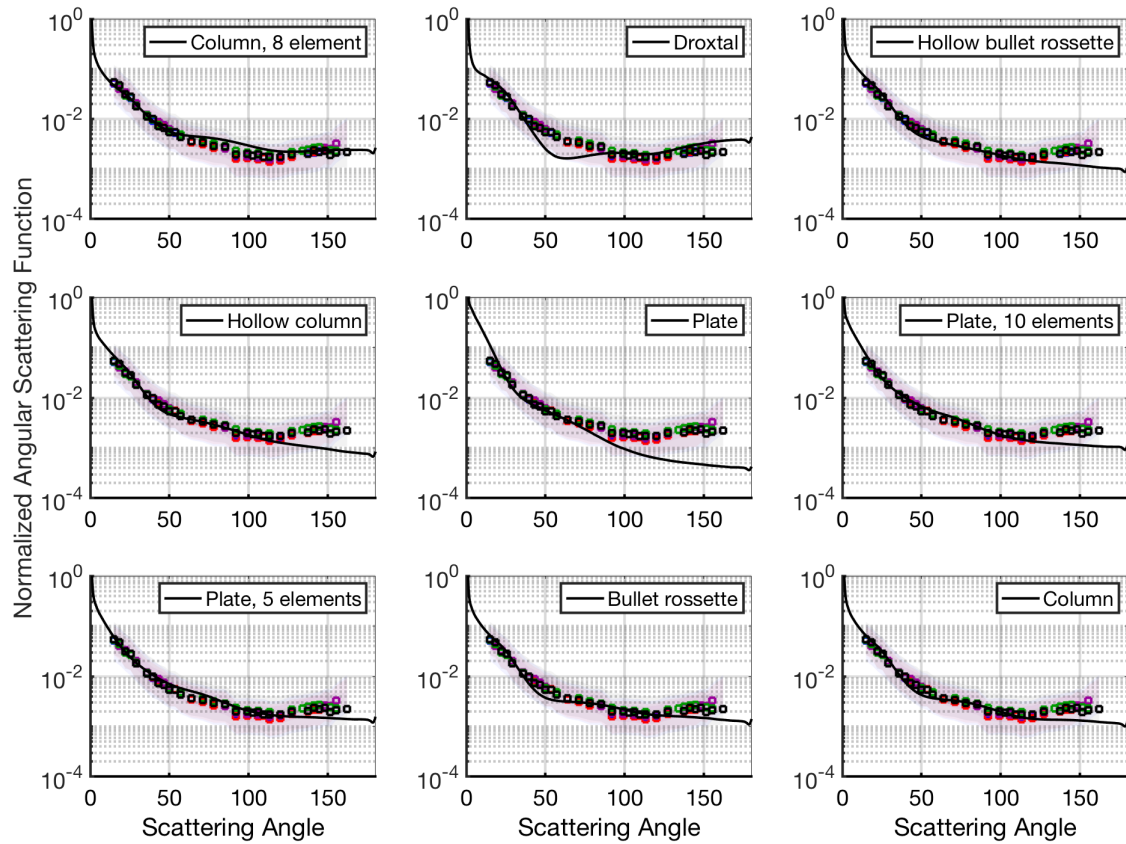


**Figure 6.** Same as Fig. 5 but now showing the comparison for PN measurements and for different optical models calculated for 804 nm. All calculations were performed assuming severely roughened surfaces. Both the measurements and the model results are normalized to the total intensity between  $15^\circ$  and  $155^\circ$ .

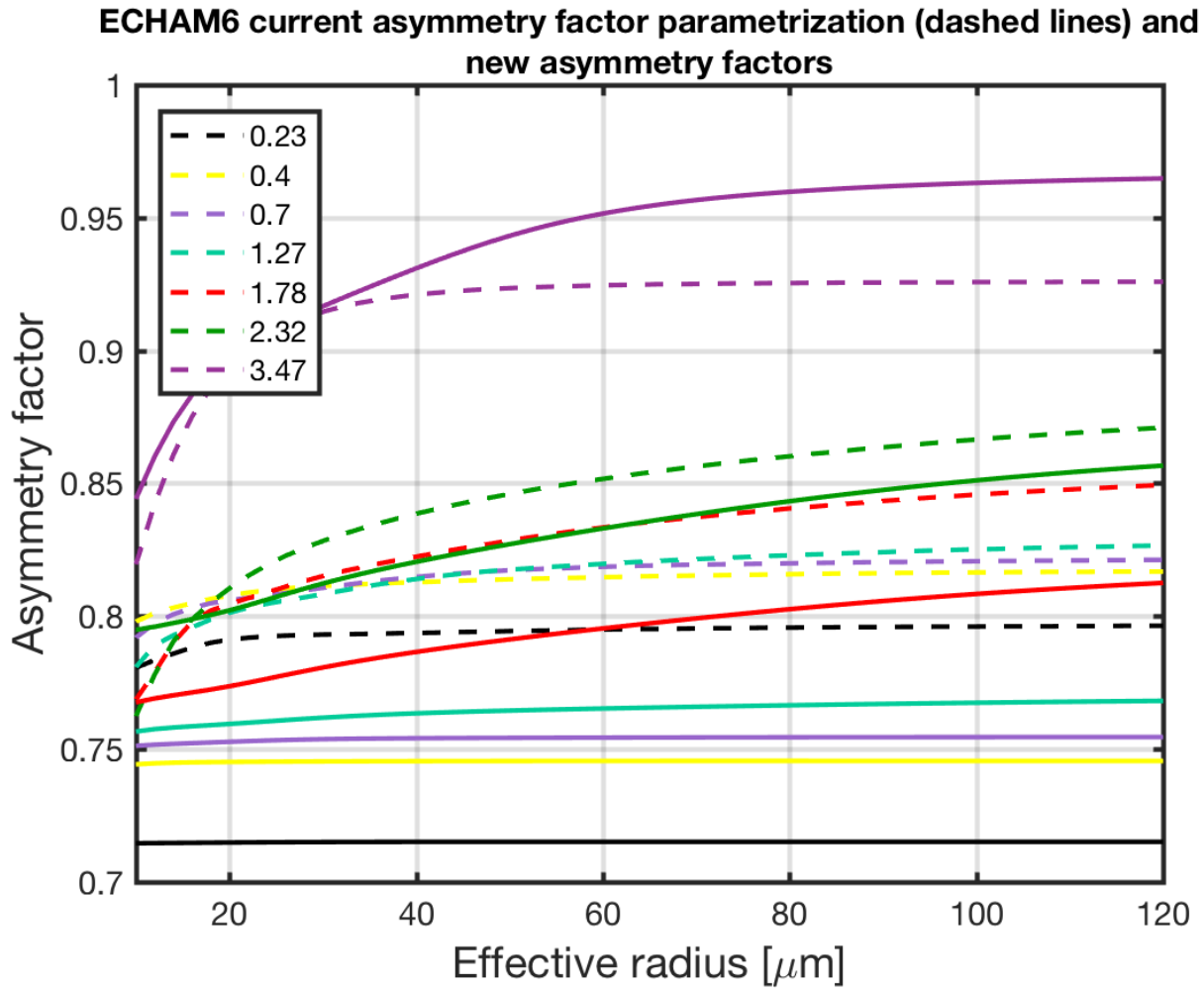


**Figure 7.** Comparison of the standard parameterization in ECHAM-HAM of the asymmetry factor of ice particle with different effective radius (dashed lines) and the new parameterization using severely roughened column aggregates (solid lines) for different wavelength bands. The wavelength bands are named with the band effective wavelength.

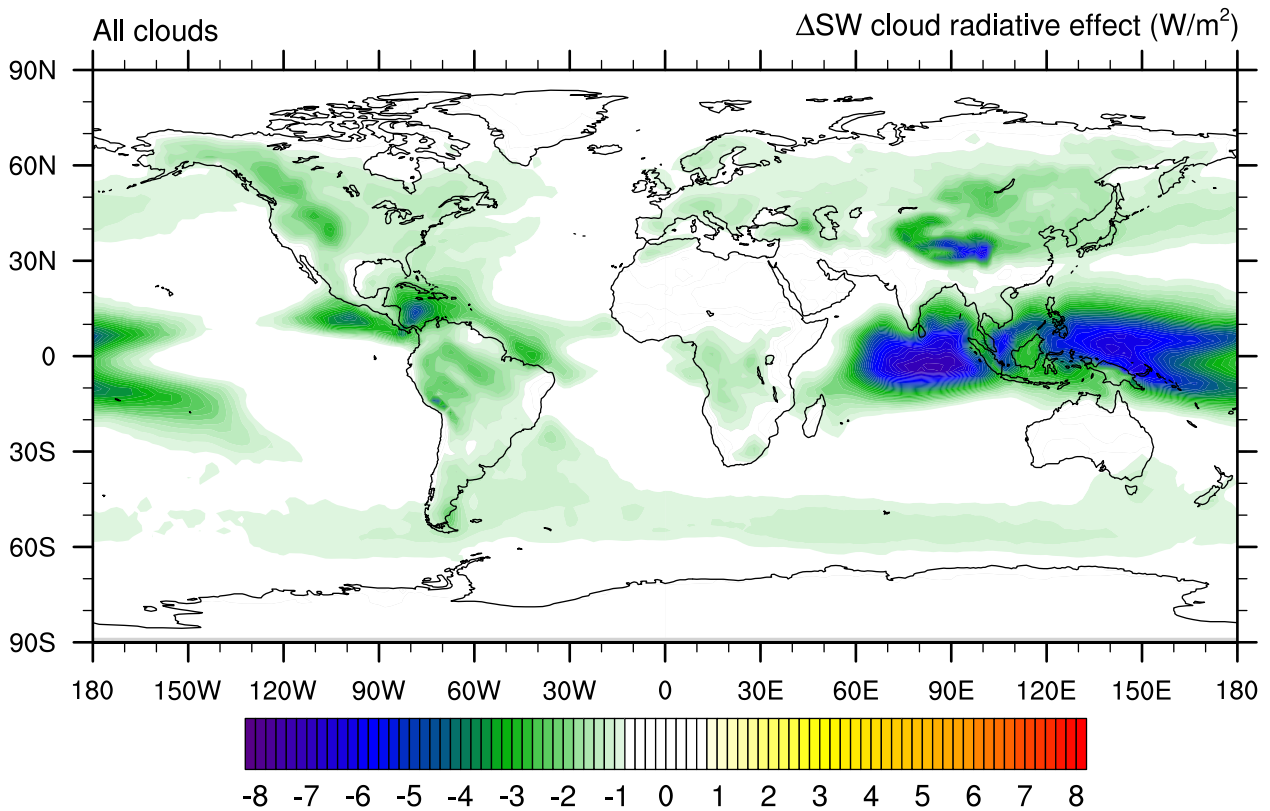


**Figure 8.** The global change in the shortwave cloud radiative effect predicted by the ECHAM-HAM model when the standard parameterization of the [short-wave short wave](#) asymmetry factor is substituted by the parameterization using severely roughened ice particles. In this simulation the new [short-wave short wave](#) asymmetry factors were applied to all ice particles both in cirrus and in mixed-phase clouds.

**Table 1.** Summary of the AIDA experiments shown in Fig. 3. The second column gives the simulated degree of complexity, the third column the AIDA campaign name and AIDA experiment number. The fourth, fifth and sixth columns give the experiment start conditions: the start temperature, the used ice nuclei (IN) and the number concentration of the aerosol acting as a cloud condensation nuclei (CCN).

	Simulated <del>submicron</del> -mesoscopic scale complexity	Campaign and experiment number	Starting temperature (K)	IN	CCN [ $\text{cm}^{-3}$ ]
AIDA hom.	severely complex	RICE03, 36	223	Sulphuric acid	105
AIDA het. 30%	severely to medium complex	RICE03, 42	223	Soot	32
AIDA het. 20%	medium complex to pristine	RICE03, 43	223	Soot	35
AIDA het. 1%	pristine	RICE02, 08	223	Soot	52

**Table 2.** Overview of the measurement campaigns. Temperature range (minimum, maximum and mean) during measurements in ice containing clouds, the operated instrumentation ~~and~~, the number of ice particles included in the analysis ~~and the percentage of ice particles rejected from the analysis owing to shattering. No particles were rejected from the SOCRATES dataset since only PHIPS datasets with manually classified images were included.~~

Campaign	$T_{min}$ (K)	$T_{max}$ (K)	$T_{mean}$ (K)	Instruments	Number of ice particles analyzed	Percentage of rejected owing
ACRIDICON	198	240	216	SID-3 & PHIPS	28,123 (SID-3 <del>analysis</del> ) & 78,177 (PHIPS <del>analysis</del> )	<del>1.33% (SID-3) &amp;</del>
MAXPEC	205	240	227	SID-3	24,769	<del>0.80</del>
ML-CIRRUS	207	241	222	SID-3	9,830	<del>0.07</del>
RACEPAC	260	273	267	SID-3	1,069	<del>19</del>
ACLOUD	256	281	271	SID-3 & PHIPS	2,812 (SID-3 <del>analysis</del> ) & 20,610 (PHIPS <del>analysis</del> )	<del>7.46% (SID-3) &amp;</del>
ARISTO 2017	215	259	239	PHIPS	9,984	<del>15.2</del>
CIRRUS'98	218	233	230	PN	2,000	
ASTAR	265	271	268	PN	2,000	
CONCERT	213	258	227	PN	4,500	
INCA NH	208	240	227	PN	22,000	
INCA SH	213	240	227	PN	32,000	
SOCRATES	238	277	251	PHIPS	107,945	